Memoirs of the Faculty of Engineering, Nagoya University
Vol. 40, No. 2 (1988)

A STUDY ON THE MULTI-MODE RESPONSE OF CONTINUOUS SYSTEMS

KIMIHIKO YASUDA and TAKAO TORII

Department of Electronic-Mechanical Engineering

(Received October 31, 1988)

Abstract

Nonlinear forced oscillations of continuous systems such as strings, membranes and beams are considered. These systems have an infinite number of natural frequencies and an infinite number of corresponding natural modes. Under some conditions, some of these modes may interact with each other, and the so-called multi-mode responses may occur. To see whether some or other types of multi-mode responses in fact occur and what their characteristics are, the oscillations induced by a periodic excitation near primary resonance points are discussed. Both theoretical and experimental analyses are conducted.

The first system taken up is a string. Its natural frequencies are in a ratio of prime integers. Due to this, oscillations containing several subharmonic or super-harmonic components occur. Thus it is shown that a type of multi-mode response occurs. The second system is a circular membrane. In this system, two modes exist in pairs with the same natural frequency and the same modal shape but are shifted circumferentially. Due to this, oscillations of rotary type occur. The third system is a square membrane. As in a circular membrane, oscillations of rotary type occur. Thus, in circular and square membranes another type of multi-mode response occurs. The last system taken up is a beam in which a natural frequency of deflectional mode and one of torsional mode are in a ratio of prime integers. It is shown that nonlinear term causes coupling between these two kinds of modes. Thus, it is shown that one more type of multi-mode response occurs.

Contents

1. Introduction

Nonlinear vibrations of continuous systems such as beams, strings, plates, membranes, and shells have been studied extensively. Eisley surveyed the nonlinear vibrations of elastic beams, rings and strings.[1] Sathyamoorthy and Pandalai surveyed the large-amplitude vibrations of discs, membranes,[2] and of plates and shells;[3] Nayfeh and Mook surveyed the nonlinear vibrations of beams, strings and plates in his excellent book;[4] Sathyamoorthy surveyed the nonlinear vibrations of plates.[5] There are also many other important studies. Some of them will be cited in relevant places in the following chapters.

Thus, so many studies have been published which treat nonlinear vibrations of continuous systems. But many of the existing studies treat free vibrations. Comparatively few studies treat forced responses. Furthermore, many of the studies treating forced responses are limited to the study of a single-mode response in which a system responds in a single natural mode. A continuous system sometimes responds, as in multi-degree-of-freedom systems, in a different way from that of a single-mode response. In fact, it responds in a form of superposition of several natural modes. This type of response is called the multi-mode response.

In multi-degree-of-freedom systems, multi-mode responses are the subjects of recent studies. Multi-degree-of-freedom system has as many natural frequencies and as many corresponding natural modes as the degrees of freedom. Under some conditions some of these modes interact with each other. This is the reason why multi-mode responses occur. One type of multi-mode response is the combination resonance which was predicted theoretically by Malkin[6] and found experimentally by Yamamoto.[7] Combination resonances have been studied by many investigators.[8-11] Another type of multi-mode response is the internal resonance. This also has been studied by many investigators.[12-21]

Continuous systems have an infinite number of natural frequencies and an infinite number of corresponding natural modes. Hence, just as in multi-degree-of-freedom systems, multi-mode responses are expected to occur. Yet, contrary to the studies in multi-degree-of-freedom systems, those in continuous systems are few.

In this study, strings, membranes, and beams are considered. It is discussed whether multi-mode responses in fact occur and what their characteristics are. The studies are both theoretical and experimental. It will be shown that in each system, one or the other types of multi-mode responses occur.

In chapter 2, strings are taken up. The strings have, as is well known, their natural frequencies in the ratio of prime integers, $1:2:3:\cdots$. Because of this, there is a possibility of the multi-mode response. It will be shown that the multi-mode responses in fact occur, and oscillations denoted by $(1/2\omega, 3/2\omega)$, etc., summed and differential harmonic oscillations, as well as almost periodic motions occur.[22-23]

In chapter 3, circular membranes are taken up. Axisymmetric oscillations of circular

membranes have already been treated, and a kind of multi-mode response is shown to occur.[24] Here oscillations in nonsymmetric case are investigated. It will be shown that here too a multi-mode response occurs, and especially oscillations of rotary type occur which have no counterpart in the axisymmetric case.[25]

In chapter 4, square membranes are taken up. In them too, oscillations of rotary type occur as well as other oscillations.[26]

In chapter 5 are considered beams, whose cross-section does not allow coupling between bending and twisting modes in a linear region. Even in such a beam, the modes may couple in a nonlinear region. Hence, a multi-mode response connected to both bending and twisting modes is expected. Here, it will be shown that this type of multi-mode response in fact occurs.

2. Multi-mode Response of a String

2. 1. Introduction

A string is a nonlinear vibratory system for large-amplitude vibration. The problems of nonlinear vibrations of a string have been treated by Carrier,[27] Oplinger,[28], Anand,[29] and others. But the investigations so far have been restricted to free vibrations. Forced oscillations are less well investigated.

As is well known, the string has its natural frequencies in the ratio of prime integers, and it is expected that the multi-mode response will occur in the string.

In this chapter, to investigate whether the multi-mode response in fact occurs in the string, oscillations near the first, second, third and fourth primary resonance points are analyzed theoretically and experimentally. The external force is supposed to consist of two components, one independent of, and the other harmonically varying with, time. For simplicity, it is assumed that oscillations occur in a plane, i.e., no spatial motions occur. In accordance with this, a thin steel strip with appropriate width is used in the experiments.

2. 2. Fundamental Equations and the Method of Solving Them

2. 2. 1. Fundamental equations

A string with length l and cross-sectional area A is considered. Origin O is fixed at one end of the string and x and y axes are taken along, and perpendicular to, the string in its equilibrium state. It is assumed that external force q acts parallel to y-axis and that deflection w occurs in the direction of force, where q and w are functions of time t as well as coordinate x. It is also assumed that a damping force acts on the string. With these assumptions, the equation of motion of the string, when the variation of tension is considered, is as follows:

$$\rho A\frac{\partial^2 w}{\partial t^2}+c\frac{\partial w}{\partial t}-\{N_0+\frac{AE}{2l}\int_0^l(\frac{\partial w}{\partial x})^2dx\}\frac{\partial^2 w}{\partial x^2}=q \tag{2.1}$$

where N_0 is the initial tension in the x-direction and where ρ, E and c are the density, Young's modulus and the damping coefficient, respectively. As mentioned above, the external force q is supposed to consist of two components, one independent of, and the

other harmonically varying with, time, i.e., it is given in the following form:

$$q=q(x)+Q(x)\cos\omega\, t \tag{2.2}$$

To rewrite Eqs. (2.1) and (2.2), a positive small parameter

$$\varepsilon=A/l^2 \tag{2.3}$$

and non-dimensional quantities

$$\left.\begin{aligned} &x'=\frac{x}{l},\quad t'=\frac{\pi}{l}\sqrt{\frac{N_0}{\rho A}}t,\quad w'=\frac{\pi}{2}\sqrt{\frac{E}{N_0}}w \\ &q'=\frac{l^2}{2\pi N_0}\sqrt{\frac{E}{N_0}}q,\quad \zeta=\frac{l^2}{2\pi A}\frac{c}{\sqrt{\rho A N_0}},\quad \omega'=\frac{\pi}{l}\sqrt{\frac{\rho A}{N_0}}\omega \end{aligned}\right\} \tag{2.4}$$

are introduced. Using these quantities and omitting primes, Eqs. (2.1) and (2.2) are transformed into

$$\frac{\partial^2 w}{\partial t^2}+2\varepsilon\zeta\frac{\partial w}{\partial t}-\frac{1}{\pi^2}\{1+\frac{2\varepsilon}{\pi^2}\int_0^1(\frac{\partial w}{\partial x})^2dx\}\frac{\partial^2 w}{\partial x^2}=q \tag{2.5}$$

$$q=q(x)+Q(x)\cos\omega\, t \tag{2.6}$$

The solution of Eq. (2.5) with the boundary conditions $w=0$ at both ends ($x=0,1$) is put in the following form:

$$w=\sum_{n=1}^{\infty}X_n\ \sin n\,\pi\, x \tag{2.7}$$

where $\sin n\,\pi\, x$ represents the n-th modal form of the string, and the coefficients X_n are an unknown function of time. Substituting Eq. (2.7) into Eq. (2.5) and applying the Galerkin method yields the equations for determining X_n as follows:

$$\frac{d^2X_n}{dt^2}+2\varepsilon\zeta\frac{dX_n}{dt}+p_n{}^2X_n+\varepsilon n^2(\sum_{m=1}^{\infty}m^2X^2{}_m)X_n=q_n+Q_n\ \cos\omega\, t \tag{2.8}$$

where

$$\left.\begin{aligned} &q_n=2\int_0^1 q(x)\sin n\,\pi\, x\, d\, x \\ &Q_n=2\int_0^1 Q(x)\sin n\,\pi\, x\, d\, x \\ &p_n=n \end{aligned}\right\} \tag{2.9}$$

2. 2. 2. Analysis by the perturbation method

To analyze oscillations near the k-th primary resonance point, it is assumed that the

detuning between ω and p_k is of the order of ε so that the exciting frequency ω can be put in the form

$$\omega = p_k + \varepsilon\sigma \tag{2.10}$$

To apply the perturbation method of multiple scales, the times with different scales, $T_0=t$, $T_1=\varepsilon t, \cdots$, are first introduced. Then, the solutions of Eq. (2.8) are put in the following form:

$$X_n = X_{n0}(T_0, T_1, \cdots) + \varepsilon X_{n1}(T_0, T_1, \cdots) + \cdots \tag{2.11}$$

It is also assumed that the external force satisfies the following conditions:

$$\left.\begin{aligned} &Q_n = \bigcirc(1) \quad (n \neq k), \quad Q_k = \bigcirc(\varepsilon) = \varepsilon Q_{k1} \\ &q_n = \bigcirc(1) \end{aligned}\right\} \tag{2.12}$$

Finally the perturbation method is applied to Eq. (2.8). Thus, the solutions are obtained, to an accuracy of order of ε, in the following form:

$$\left.\begin{aligned} X_{k0} &= A_k \ e^{i p_k T_0} + \overline{A}_k \ e^{-i p_k T_0} + D_k \\ X_{n0} &= A_n \ e^{i p_n T_0} + \overline{A}_n \ e^{-i p_n T_0} \\ &\quad + \frac{1}{2} P_n (e^{i \omega T_0} + e^{-i \omega T_0}) + D_n \quad (n \neq k) \end{aligned}\right\} \tag{2.13}$$

where

$$\left.\begin{aligned} &P_n = Q_n / (p_n{}^2 - \omega^2) \quad (n \neq k) \\ &D_n = q_n / p_n{}^2 \end{aligned}\right\} \tag{2.14}$$

and where A_n are unknown functions of T_1, with $\overline{A}_n$ being conjugate to A_n. The functions A_n and $\overline{A}_n$ are determined by the conditions that X_n do not contain secular terms, i.e., the conditions

$$\left.\begin{aligned} &2 i p_k A_k' + 2 i p_k \zeta A_k - \frac{1}{2} Q_{k1} \ e^{i \sigma T_1} \\ &\quad + k^2 \{ \sum_{m=1}^{\infty} m^2 (2 A_m \overline{A}_m) + \cdots \} A_k + \cdots = 0 \\ &2 i p_n A_n' + 2 i p_n \zeta A_n \\ &\quad + n^2 \{ \sum_{m=1}^{\infty} m^2 (2 A_m \overline{A}_m) + \cdots \} A_n + \cdots = 0 \quad (n \neq k) \end{aligned}\right\} \tag{2.15}$$

where symbol $'$ means differentiation with respect to T_1. For numerical calculation, quantities A_n, P_n, D_n with $n>3$ are neglected and the first equation as well as the second equations for $n=1,3$ are retained. Such a treatment is, as will be shown later, enough for

explaining the experimental results.

2. 2. 3. Occurrence of oscillations containing several super-harmonic oscillations or subharmonic oscillations

To solve Eq. (2.15), unknown quantities A_n are put in the form

$$A_n=\frac{1}{2}R_n\ e^{i(\frac{n}{k}\sigma T_1-\gamma_n)} \tag{2.16}$$

and are substituted into Eq. (2.15). Dividing the resulting equations into real an imaginary parts, yields equations of the form

$$\left.\begin{aligned}
&p_kR_k'=-p_k\zeta R_k+\frac{1}{2}Q_{k1}\sin\gamma_k+\cdots\\
&p_kR_k\,\gamma_k'=p_k\sigma R_k+\frac{1}{2}Q_{k1}\cos\gamma_k\\
&\qquad\qquad -k^2\{\sum_{m=1}^{\infty}m^2(\frac{1}{4}R_m^2)+\cdots\}R_k+\cdots\\
&p_nR_n'=-p_n\zeta R_n+\cdots \qquad (n\neq k)\\
&p_nR_n\,\gamma_n'=\frac{n}{k}p_n\sigma R_n-n^2\{\sum_{m=1}^{\infty}m^2(\frac{1}{4}R_m^2)+\cdots\}R_n+\cdots \qquad (n\neq k)
\end{aligned}\right\} \tag{2.17}$$

Solving these equations for R_n and γ_n and substituting the results into Eq. (2.16) and then into Eqs. (2.13) and (2.7), yields the deflection w in the form:

$$w=\sum_{n=1}^{\infty}\{R_n\cos(\frac{n}{k}\omega\ t-\gamma_n)+P_n\cos\omega\ t+D_n\}\sin n\ \pi\ x \tag{2.18}$$

where $P_k=0$.

To determine steady-state oscillations for deflection w, constant solutions of Eq. (2.17) satisfying the conditions

$$R_n'=0,\ \gamma_n'=0 \tag{2.19}$$

are obtained.

Among constant solutions of Eq. (2.17) satisfying the conditions (2.19), the solutions satisfying $R_k\neq0$, $R_n=0$ $(n\neq k)$ imply, as can be seen from Eq. (2.18), the occurrence of a harmonic oscillation in the k-th mode shape. On the other hand, if the solutions satisfying $R_n\neq0$, $(n\neq k)$ exist, then these solutions imply the occurrence of oscillations containing the n-th super-harmonic oscillation (for $k=1$) or n/k-th subharmonic oscillation (for $k\neq1$), each in the n-th mode shape.

To determine the stability of a steady-state oscillation, it is necessary to determine the stability of the corresponding constant solution. The stability of the constant solution

denoted by A_n is determined by giving it a slight disturbance Δ_n and examine its variation with respect to time. To examine this, equations for determining Δ_n are obtained by substituting $A_n+\Delta_n$ in place of A_n in Eq. (2.15) and by neglecting small quantities higher than the second order of Δ_n. Then, in the resulting equations, Δ_n in the form

$$\Delta_n=(\xi_n+i\,\eta_n)\;\; e^{i\frac{n}{k}\sigma T_1} \tag{2.20}$$

and also A_n in the form

$$A_n=\frac{1}{2}(u_n+i\,v_n)\;\; e^{i\frac{n}{k}\sigma T_1} \tag{2.21}$$

are substituted. Finally, dividing the resulting equations into real and imaginary parts, yields variational equations in terms of ξ_n and η_n with real coefficients. Applying the Routh-Hurwitz criterion to these final equations, determines the required stability.

Equations (2.17) sometimes have, in addition to constant solutions, periodic solutions with R_n and γ_n varying in an equal time interval. This type of solution implies, as can be seen from Eq. (2.18), the occurrence of almost periodic motions. This type of oscillation is obtained by integrating Eq. (2.17) numerically with a suitable initial condition until a periodic solution is reached.

Equations (2.17) are a set of infinite number of equations which cannot be solved strictly. Here only a finite number of equations are retained for numerical analysis. It is shown, by comparing with experimental results, that such a treatment is enough for qualitative discussion.

2. 3. *Experimental method*

A schematic diagram of the experimental apparatus used in this study is shown in Fig. 2. 1. In the figure, B denotes the string. Initial tension N_0 is given to the string by tightening the nut shown in the left side in the figure. The periodic exciting force is given to the string by the current flowing alternately to two electromagnets M_1 and M_2 placed

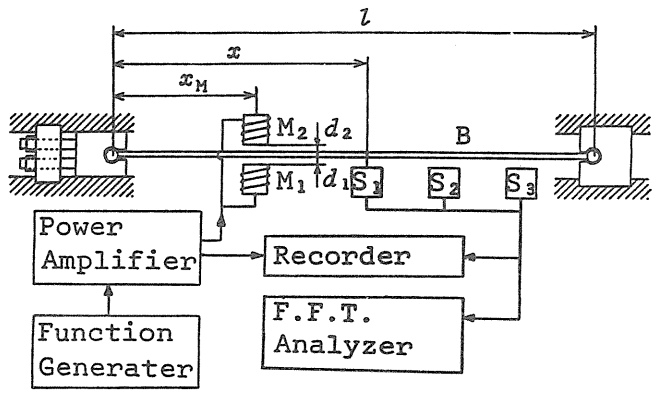

Fig. 2. 1. Schematic diagram of the experimental apparatus.

on both sides of the string. By varying the distances d_1 and d_2 of the electromagnets from the string, a constant component can be included in the exciting force. The oscillation induced in the string are measured by three sensors S_1, S_2 and S_3 placed as shown in the figure. The amplitudes of each component of the deflection are determined by calculating the weighted mean of amplitudes obtained by spectrum analysis of the deflections at chosen points.

The dimensions of the string and its properties are as follows:

length	$l=816$ mm	
width	$b=19$ mm	
thickness	$h=0.5$ mm	(2.22)
Young's modulus	$E=206$ GPa	
density	$\rho=7.84\times10^3$ Kg/m^3	

The natural frequencies of the string change with initial tension and the obtained values in the experiment are as follows:

$$p_1=26.0\text{ Hz},\quad p_2=52.0\text{ Hz}$$
$$p_3=78.0\text{ Hz},\quad p_4=105.5\text{ Hz} \tag{2.23}$$

Here and in what follows, the same notations are used to denote the frequencies instead of angular frequencies. The natural frequencies in Eq. (2.23) are approximately in the ratio of integer and the steel strip used in the experiment can be regarded as a string.

2. 4. *Oscillations Near the First Primary Resonance Point*

2. 4. 1. *Occurrence of superharmonic oscillation*

The response near the first primary resonance point is obtained by putting $k=1$ in the analysis given in Sect. 2. 2. 3. For numerical analysis, the first three modes are retained. Hence the six equations governing R_n, γ_n ($n=1,2,3$), or the equivalent, are used in Eq. (2.17), with R_n, P_n, D_n ($n>3$) neglected. Eq. (2.17) for this case is

$$\begin{aligned}
p_1R_1' &= -p_1\zeta R_1+\frac{1}{2}Q_{11}\sin\gamma_1-\frac{1}{8}R_1\sum_{m=1}^{3}m^2P_m^2\sin2\gamma_1\\
&\quad -D_1\sum_{m=1}^{3}m^2D_mP_m\sin\gamma_1-2D_1P_2R_2\sin(\gamma_1-\gamma_2)\\
&\quad -2D_2R_2R_1\sin(2\gamma_1-\gamma_2)-\frac{9}{4}P_3R_3R_1\sin(2\gamma_1-\gamma_3)\\
p_1R_1\gamma_1' &= p_1\sigma R_1+\frac{1}{2}Q_{11}\cos\gamma_1\\
&\quad -\{\sum_{m=1}^{3}m^2(\frac{1}{4}R_m^2+\frac{1}{4}P_m^2+\frac{1}{2}D_m^2)+\frac{1}{8}R_1^2+\frac{1}{2}P_1^2+D_1^2\}R_1\\
&\quad -\frac{1}{8}R_1\sum_{m=1}^{3}m^2P_m^2\cos2\gamma_1-D_1\sum_{m=1}^{3}m^2D_mP_m\cos\gamma_1\\
&\quad -2D_1P_2R_2\cos(\gamma_1-\gamma_2)-2D_2R_2R_1\cos(2\gamma_1-\gamma_2)\\
&\quad -\frac{9}{4}P_3R_3R_1\cos(2\gamma_1-\gamma_3)
\end{aligned}$$

$$
\left.
\begin{aligned}
p_2R_2' &= -p_2\zeta R_2 - 2D_1P_2R_1\sin(\gamma_2-\gamma_1) - D_2R_1^2\sin(\gamma_2-2\gamma_1) \\
&\quad -9P_3R_3R_2\sin(2\gamma_2-\gamma_3) - 18(D_2P_3+D_3P_2)R_3\sin(\gamma_2-\gamma_3) \\
&\quad -(2P_2\sum_{m=1}^{3}m^2D_mP_m + D_2\sum_{m=1}^{3}m^2P_m^2)\sin\gamma_2 \\
p_2R_2\gamma_2' &= 2p_2\sigma R_2 \\
&\quad -4\{\sum_{m=1}^{3}m^2(\frac{1}{4}R_m^2+\frac{1}{4}P_m^2+\frac{1}{2}D_m^2)+\frac{4}{8}R_2^2+\frac{4}{2}P_2^2+4D_2^2\}R_2 \\
&\quad -2D_1P_2R_1\cos(\gamma_2-\gamma_1) - D_2R_1^2\cos(\gamma_2-2\gamma_1) \\
&\quad -9P_3R_3R_2\sin(2\gamma_2-\gamma_3) - 18(D_2P_3+D_3P_2)R_3\cos(\gamma_2-\gamma_3) \\
&\quad -(2P_2\sum_{m=1}^{3}m^2D_mP_m + D_2\sum_{m=1}^{3}m^2P_m^2)\cos\gamma_2 \\
p_3R_3' &= -p_3\zeta R_3 - \frac{9}{8}P_3R_2^2\sin(\gamma_3-2\gamma_1) - \frac{9}{8}P_3\sum_{m=1}^{3}m^2P_m^2\sin\gamma_3 \\
&\quad -\frac{9}{2}P_3R_2^2\sin(\gamma_3-2\gamma_2) - 18(D_2P_3+D_3P_2)R_2\sin(\gamma_3-\gamma_2) \\
p_3R_3\gamma_3' &= 3p_3\sigma R_3 \\
&\quad -9\{\sum_{m=1}^{3}m^2(\frac{1}{4}R_m^2+\frac{1}{4}P_m^2+\frac{1}{2}D_m^2)+\frac{9}{8}R_3^2+\frac{9}{2}P_3^2+9D_3^2\}R_3 \\
&\quad -\frac{9}{8}P_3R_1^2\cos(\gamma_3-2\gamma_1) - \frac{9}{8}P_3\sum_{m=1}^{3}m^2P_m^2\cos\gamma_3 \\
&\quad -\frac{9}{2}P_3R_2^2\cos(\gamma_3-2\gamma_2) - 18(D_2P_3+D_3P_2)R_2\cos(\gamma_3-\gamma_2)
\end{aligned}
\right\} \quad (2.24)
$$

2. 4. 2. Characteristics of super-harmonic oscillation

An example of the response curves obtained theoretically is shown in Fig. 2. 2. In the figure, R_1 is the amplitude of the harmonic oscillation and R_2 and R_3 are the amplitudes of the second and third super-harmonic oscillations, respectively. The solid and dotted lines of the response curves (and of the response curves in the following) denote stable and unstable oscillations, respectively. In what follows, we confine our attention to the stable oscillations.

As can be seen, the oscillations near the first primary resonance point are always accompanied with more or less super-harmonic oscillations. They are classified into two types. To one belong oscillations denoted by branches O_0 and O_2 which are accompanied with small super-harmonic oscillations. To the other belong oscillations denoted by branches A, A′ and B which are accompanied with large super-harmonic oscillations. The former can be regarded as the usual harmonic oscillations, but the latter are special types of oscillations. The oscillations denoted by branches A and A′ are those whose phase difference γ_2 is nearly π.

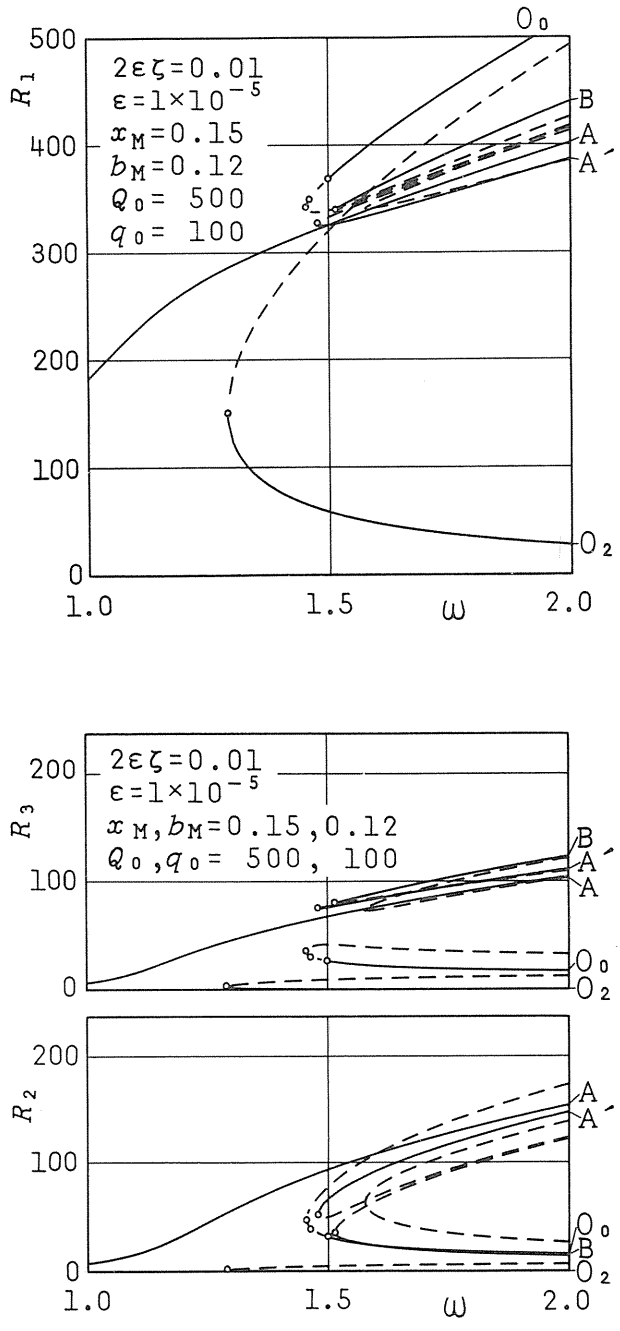

Fig. 2. 2. Response curves obtained theoretically near the first primary resonance point.

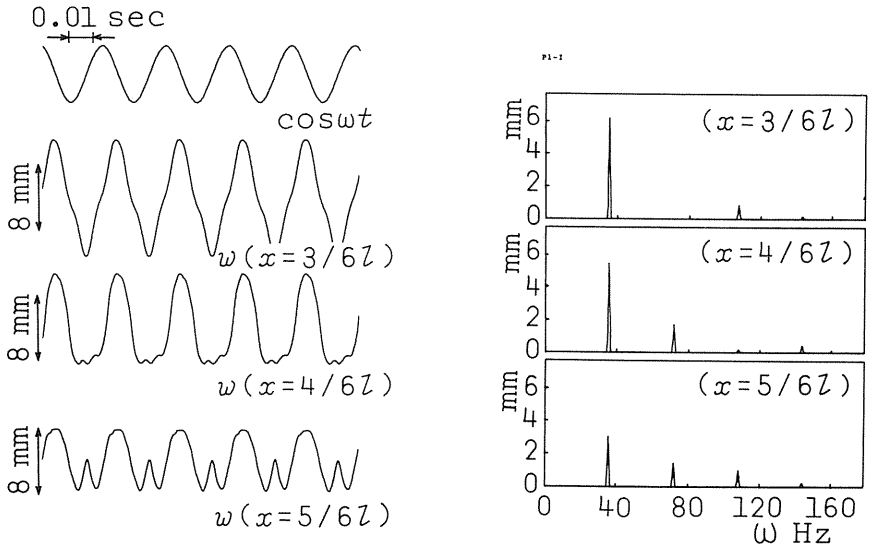

(a) The oscillation shown by a symbol △ in the Fig. 2. 4 (36 Hz).

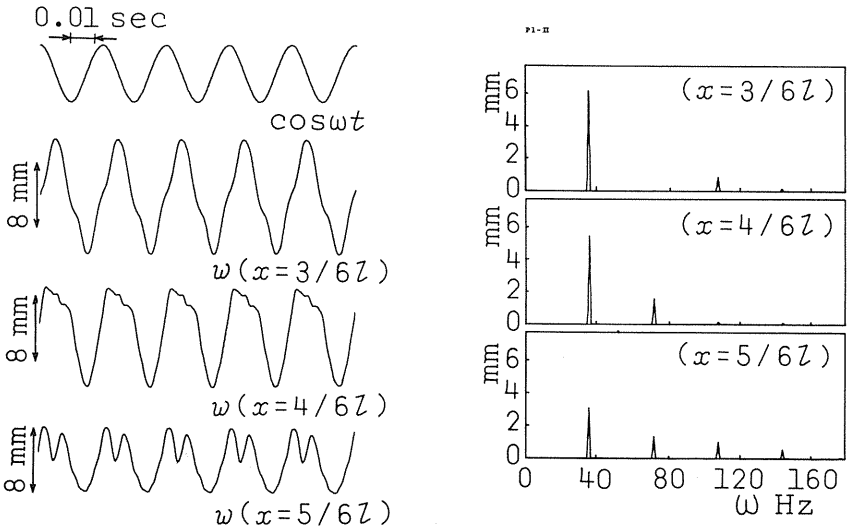

(b) The oscillation shown by a symbol ▽ in the Fig. 2. 4 (36 Hz).

Fig. 2. 3. Waveform and spectrum of oscillation near the first primary resonance point.

When the excitation frequency ω increases gradually from a low value, the oscillations denoted by A occur. But, as the branches other than A separate from branch A, the oscillations denoted by these branches do not occur spontaneously, but occur only when appropriate initial conditions are given. In the region of high frequencies, several branches exist, and which oscillation occurs, depends on the initial conditions.

2. 4. 3. Experimental results

Near the first primary resonance point were observed experimentally the occurrences of such oscillations as shown in Fig. 2. 3. In the figures, the left figure shows the time variation of the deflection and the right the result of its spectrum analysis with its constant component omitted. As seen from the figures, the oscillations contain the super-harmonic oscillations as their components. By comparing the waveforms in Figs. (a) and (b), it is found that the phase of the second super-harmonic oscillations are different from each other nearly by π.

The response curves obtained experimentally are shown in Fig. 2. 4. In the figure, ○ denotes the oscillations containing small super-harmonic oscillations. △ and ▽ denote those shown in Fig. 2. 3 (a), and those shown in Fig. 2. 3 (b), respectively. The oscillations denoted by △ occur spontaneously as ω increases, but those denoted by ▽ occur only when an appropriate shock is given to the string. From these facts it is seen that the oscillations denoted by △ and ▽ correspond to the ones denoted by A and A′ in Fig. 2. 2, respectively. The oscillations which correspond to those denoted by B in Fig. 2. 2 did not occur in the experiment. Thus, the experimental results confirm well the validity of the theoretical analysis.

2. 5. Oscillations near the second primary resonance point

2. 5. 1. Occurrence of subharmonic oscillations

The response near the second primary resonance point is obtained by putting $k=2$ in

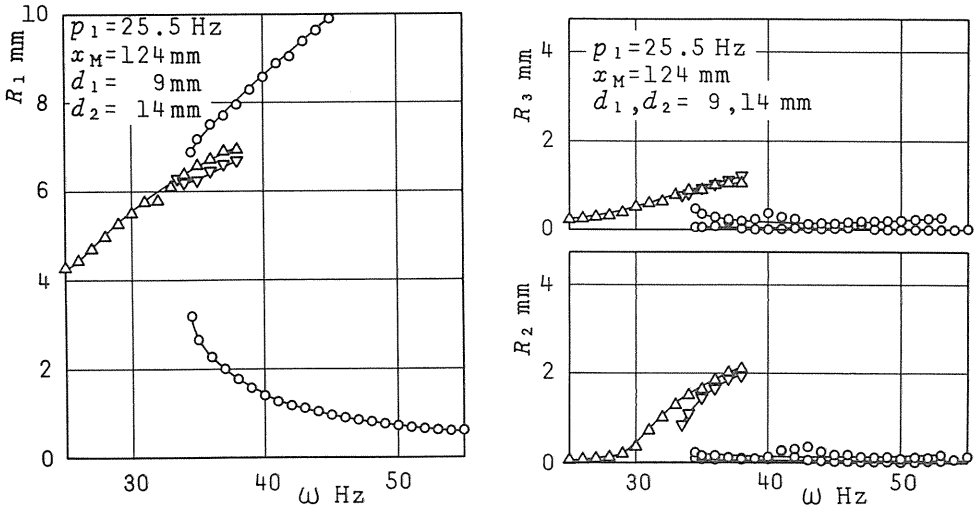

Fig. 2. 4. Response curves obtained experimentally near the first primary resonance point.

the analysis given in Sect. 2. 2. 3. For numerical analysis, the first three modes are retained. Hence the six equations governing R_n, γ_n (n=1,2,3), or the equivalent, are used in Eq. (2.17), with R_n, P_n, D_n (n>3) neglected. Eq. (2.17) for this case is

$$
\left.
\begin{aligned}
p_1R_1' &= -p_1\zeta R_1 \\
&\quad -2D_2R_2R_1\sin(2\gamma_1-\gamma_2)-(\frac{1}{2}\sum_{m=1}^{3}m^2D_mP_m+D_1P_1)R_1\sin 2\gamma_1 \\
&\quad -\frac{9}{4}P_1P_3R_3\sin(\gamma_1+\gamma_3)-\frac{9}{2}(D_1P_3+D_3P_1)R_3\sin(\gamma_1-\gamma_3) \\
p_1R_1\gamma_1' &= \frac{1}{2}p_1\sigma R_1 \\
&\quad -\{\sum_{m=1}^{3}m^2(\frac{1}{4}R_m^2+\frac{1}{4}P_m^2+\frac{1}{2}D_m^2)+\frac{1}{8}R_1^2+\frac{1}{2}P_1^2+D_1^2\}R_1 \\
&\quad -2D_2R_2R_1\cos(2\gamma_1-\gamma_2)-(\frac{1}{2}\sum_{m=1}^{3}m^2D_mP_m+D_1P_1)R_1\cos 2\gamma_1 \\
&\quad -\frac{9}{4}P_1P_3R_3\cos(\gamma_1+\gamma_3)-\frac{9}{2}(D_1P_3+D_3P_1)R_3\cos(\gamma_1-\gamma_3) \\
p_2R_2' &= -p_2\zeta R_2+\frac{1}{2}Q_{21}\sin\gamma_2-D_2R_1^2\sin(\gamma_2-2\gamma_1) \\
&\quad -\frac{4}{8}R_2\sum_{m=1}^{3}m^2P_m^2\sin 2\gamma_2-4D_2\sum_{m=1}^{3}m^2D_mP_m\sin\gamma_2 \\
p_2R_2\gamma_2' &= \frac{2}{2}p_2\sigma R_2+\frac{1}{2}Q_{21}\cos\gamma_2-D_2R_1^2\cos(\gamma_2-2\gamma_1) \\
&\quad -4\{\sum_{m=1}^{3}m^2(\frac{1}{4}R_m^2+\frac{1}{4}P_m^2+\frac{1}{2}D_m^2)+\frac{4}{8}R_2^2+\frac{4}{2}P_2^2+4D_2^2\}R_2 \\
&\quad -\frac{4}{8}R_2\sum_{m=1}^{3}m^2P_m^2\cos 2\gamma_2-4D_2\sum_{m=1}^{3}m^2D_mP_m\cos\gamma_2 \\
p_3R_3' &= -p_3\zeta R_3 \\
&\quad -\frac{9}{4}P_1P_3R_1\sin(\gamma_3+\gamma_1)-\frac{9}{2}(D_1P_3+D_3P_1)R_1\sin(\gamma_3-\gamma_1) \\
p_3R_3\gamma_3' &= \frac{3}{2}p_3\sigma R_3 \\
&\quad -9\{\sum_{m=1}^{3}m^2(\frac{1}{4}R_m^2+\frac{1}{4}P_m^2+\frac{1}{2}D_m^2)+\frac{9}{8}R_3^2+\frac{9}{2}P_3^2+9D_3^2\}R_3 \\
&\quad -\frac{9}{4}P_1P_3R_1\cos(\gamma_3+\gamma_1)-\frac{9}{2}(D_1P_3+D_3P_1)R_1\cos(\gamma_3-\gamma_1)
\end{aligned}
\right\} \quad (2.25)
$$

The steady-state solutions of Eq. (2.25) can be classified into two groups, one with R_1=R_3=0 and the other with $R_1\neq 0$, $R_3\neq 0$. The former solutions imply occurrence of the harmonic oscillation, and the latter that of the oscillation containing subharmonic

oscillations of orders 1/2 and 3/2. The latter oscillation will be called in this paper, with use of its components, the oscillation of type $(1/2\omega,\ 3/2\omega)$.

2. 5. 2. Characteristics of subharmonic oscillations

An example of the response curves obtained theoretically is shown in Fig. 2. 5. In the figure, R_2 is the amplitude of the harmonic oscillation and R_1 and R_3 are the amplitudes of the subharmonic oscillations of orders 1/2 and 3/2, respectively.

In the figure it is seen that the response curve consists, as mentioned above, of two kinds of branches. To one belong the branches O_0, O_2 representing the harmonic oscillations and to the other, the branches representing the oscillation of type $(1/2\omega,\ 3/2\omega)$. On the former branch O_0 exists an unstable portion, and from its boundary points the latter branches bifurcate. Of the latter branches, the branch A which bifurcates from the lower boundary point is stable. Thus with an increase of the exciting angular frequency ω, a transition occurs from the state of occurrence of the harmonic oscillation to the state of occurrence of the oscillation of type $(1/2\omega,\ 3/2\omega)$. Of the branches of the oscillation of type $(1/2\omega,\ 3/2\omega)$, the branches A and B are stable. The latter branch B is such that R_3 is small, and hence this branch represents in effect the occurrence of the usual subharmonic oscillation of order 1/2.

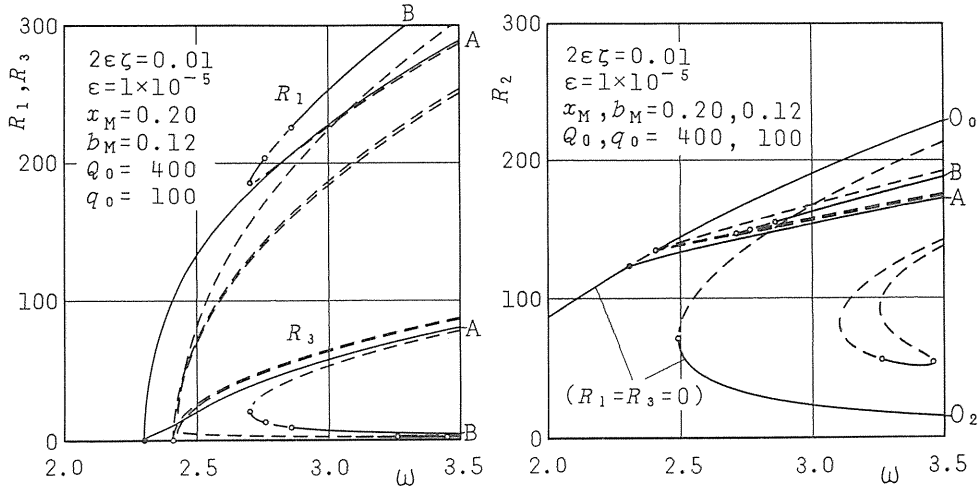

Fig. 2. 5. Response curves obtained theoretically near the second primary resonance point $(q_0\neq0)$.

2. 5. 3. Occurrence of summed and differential harmonic oscillations

In the previous section, the case with presence of $q(x)\neq0$ was considered. Here the case with $q(x)=0$ or $q(x)$ being small of the order of ε, is taken up. With this condition the quantities D_n in Eq. (2.25) become zero, and the unknown quantities γ_1 and γ_3 always appear in Eq. (2.25) in the form $(\gamma_1+\gamma_3)$. Hence the steady-state solutions determined by

conditions (2.19) generally do not exist, and hence the oscillation containing several subharmonic oscillations cannot occur.

To examine what steady-state oscillations then occur, the second and the sixth equations in Eq. (2.25) are combined to yield

$$\begin{aligned} p_1p_3R_1R_3\gamma_{13}' &= 2p_1p_3\sigma R_1R_3 \\ &-p_3\{\sum_{m=1}^{3} m^2(\frac{1}{4}R_m^2+\frac{1}{4}P_m^2)+\frac{1}{8}R_1^2+\frac{1}{2}P_1^2\}R_1R_3 \\ &-9p_1\{\sum_{m=1}^{3} m^2(\frac{1}{4}R_m^2+\frac{1}{4}P_m^2)+\frac{9}{8}R_3^2+\frac{9}{2}P_3^2\}R_1R_3 \\ &-\frac{9}{4}P_1P_3(p_1R_1^2+p_3R_3^2)\cos\gamma_{13} \end{aligned} \tag{2.26}$$

where $\gamma_{13}=\gamma_1+\gamma_3$. Then it is assumed that the constant solutions are given by the conditions

$$R_1'=R_2'=R_3'=0,\ \gamma_2'=\gamma_{13}'=0 \tag{2.27}$$

For these conditions, the solutions for R_n, γ_2 and γ_{13} do exist. Substituting them yields the deflection in the form of Eq. (2.18).

The solution of Eq. (2.25) with condition (2.27) can be classified into two groups, one with $R_1=R_3=0$ and the other with $R_1\neq0$, $R_3\neq0$. The former solution implies the occurrence of the usual harmonic oscillation. To see what the latter solution implies, the angular frequencies ω_1 and ω_3 of the first and third mode components are examined. From Eq. (2.18) it is seen that

$$\omega_1=\frac{1}{2}\omega-\gamma_1',\ \omega_3=\frac{3}{2}\omega-\gamma_3' \tag{2.28}$$

In the above expressions the values of γ_1' and γ_3' are given by Eq. (2.17). Because $\gamma_1'\neq0$ and $\gamma_3'\neq0$ hold generally, ω_1 and ω_3 are not in a simple relation with ω. However, from condition $\gamma_{13}'=0$ in Eq. (2.27), it is seen that

$$\omega_1+\omega_3=2\omega \tag{2.29}$$

Hence, the present oscillation represents the summed and differential harmonic oscillation. Thus, the solution with $R_1\neq0$ and $R_3\neq0$ implies the occurrence of the summed and differential harmonic oscillation.

2. 5. 4. Characteristics of summed and differential harmonic oscillations

An example of the response curves obtained for $q_0=0$ is shown in Fig. 2. 6. In the figure, R_2 is the amplitude of the harmonic oscillation and R_1 and R_3 are the amplitudes of the summed and differential harmonic oscillations, respectively. The angular frequencies of the summed and differential harmonic oscillations are given in Fig. 2. 7. In the figure are added, for comparison, chain lines expressing 1/2 times and 3/2 times the

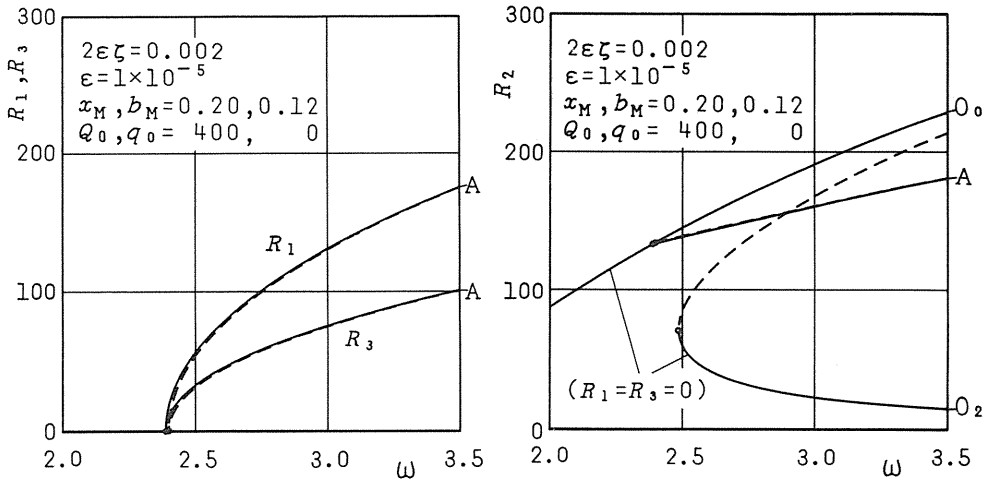

Fig. 2. 6. Response curves obtained theoretically near the second primary resonance point ($q_0=0$).

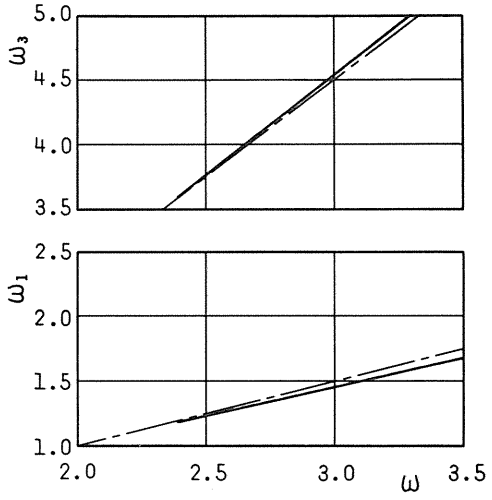

Fig. 2. 7. Frequencies of the components in the summed and differential harmonic oscillation.

exciting frequency.

The curves in Fig. 2. 6 consists of two kinds of branches. To one belong branches O_0, O_2 representing the harmonic oscillation and to the other, branches representing the summed and differential harmonic oscillation. On the former branch O_0 exists an unstable portion, and from its boundary points the latter branches bifurcate. Of these branches, the branch A bifurcating from the lower boundary point is stable. Thus, with an increases of exciting frequency ω, a transition occurs from the state of occurrence of the harmonic oscillation to the state of occurrence of the summed and differential harmonic oscillation.

2. 5. 5. Experimental results

In the experiment with the condition $d_1 \neq d_2$, we observed that such an oscillation occurred as is shown in Fig. 2. 8, in which the left figure shows the time variation of

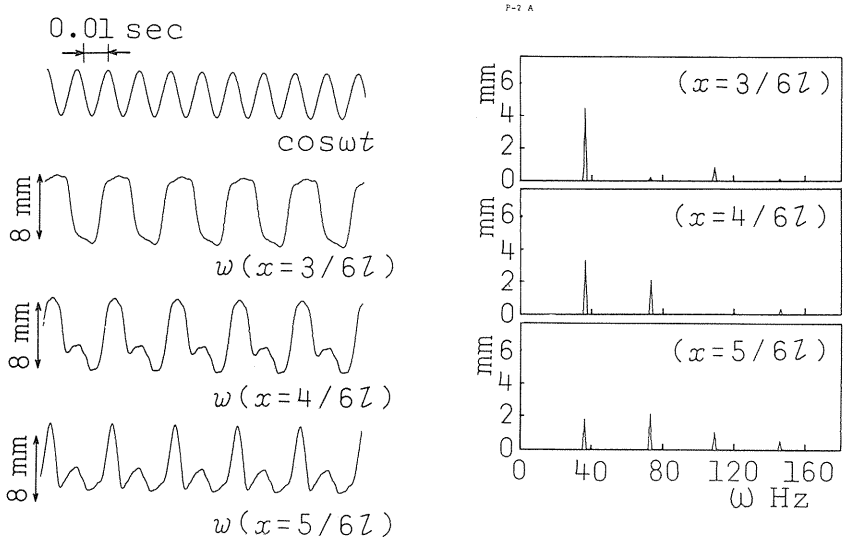

(a) The oscillation of type (1/2ω, 3/2ω) (73 Hz).

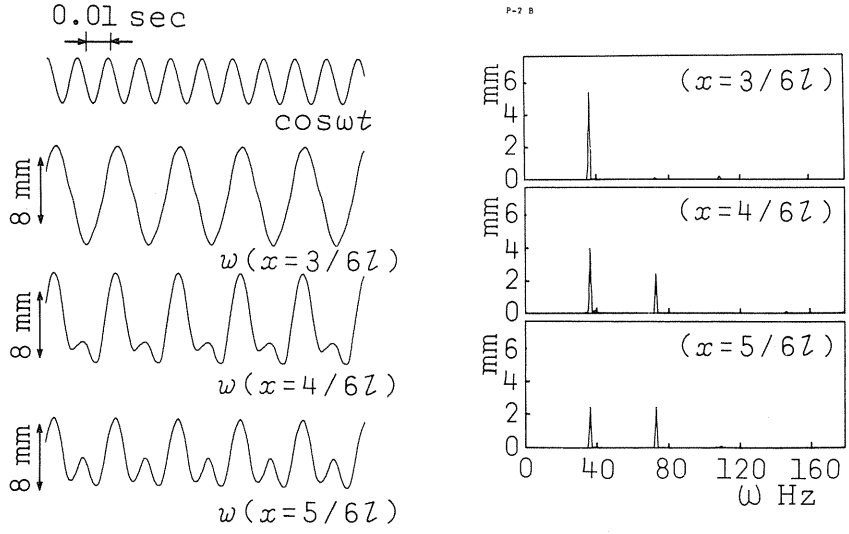

(b) Subharmonic oscillation of order 1/2 (73 Hz).

Fig. 2. 8. Waveform and spectrum of oscillation near the second primary resonance point ($d_1 \neq d_2$).

deflection and the right figure the result of its spectrum analysis. The figure indicates that the oscillation contains components with frequencies $1/2\omega$, ω, $3/2\omega$ and that these components take the first, second and third modal shapes, respectively. Thus, it was confirmed experimentally that the oscillation of type ($1/2\omega$, $3/2\omega$) occurred.

The response curve obtained experimentally is shown in Fig. 2. 9. In the figure, ○ shows occurrence of the harmonic oscillation and ● the occurrence of the oscillation of type ($1/2\omega$, $3/2\omega$). It is seen from the figure that the branch of the harmonic oscillation contains an unstable portion, and from its boundaries the branches of the oscillation of type ($1/2\omega$, $3/2\omega$) bifurcate. It is also seen that a branch exists which corresponds to branch B with small R_3 in Fig. 2. 5. These experimental results agree well with the results of the theoretical analysis.

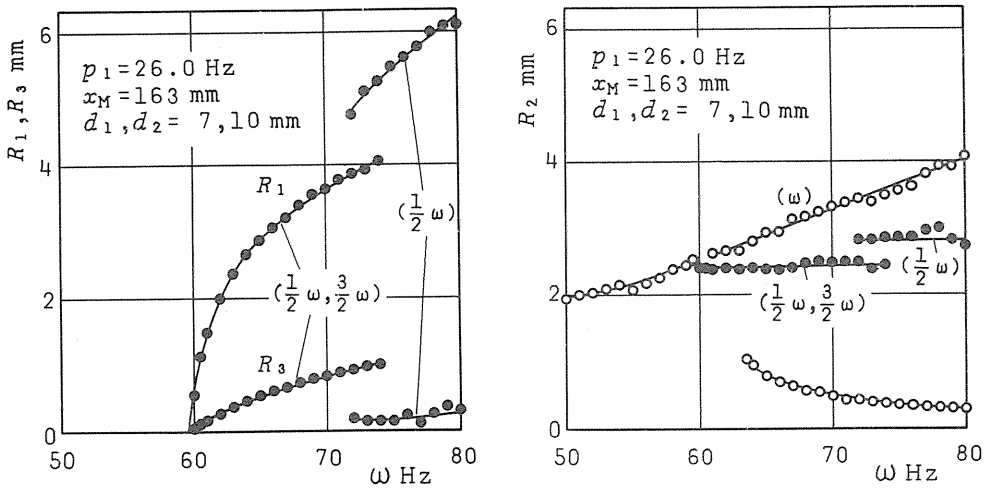

Fig. 2. 9. Response curves obtained experimentally near the second primary resonance point ($d_1 \neq d_2$).

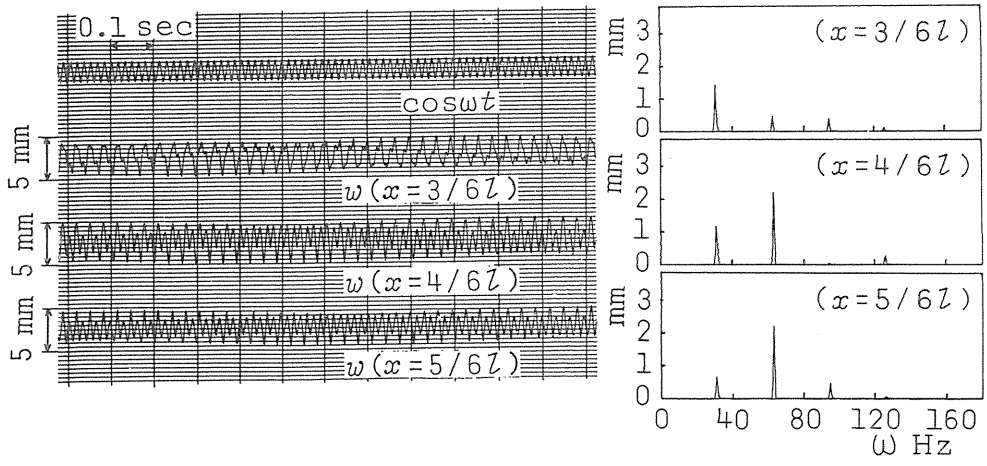

Fig. 2. 10. Waveform and spectrum of the summed and differential harmonic oscillation ($d_1 = d_2$).

Next, under the state of occurrence of the oscillation of type (1/2ω, 3/2ω), we moved the magnets so that the component q_0 became small while keeping (d_1+d_2) at a constant value. In doing this, we observed that the oscillation of type (1/2ω, 3/2ω) disappeared, and appeared such an oscillation as is shown in Fig. 2. 10, in which the left figure shows the time variation and the right figure the result of spectrum analysis. In the figure it is seen that the oscillation contains, in addition to the harmonic oscillation, oscillations with frequencies ω_1 and ω_3. Also it is seen that the later oscillations take the form of the first and third modal shapes, and that the frequencies ω_1 and ω_3 satisfy the condition

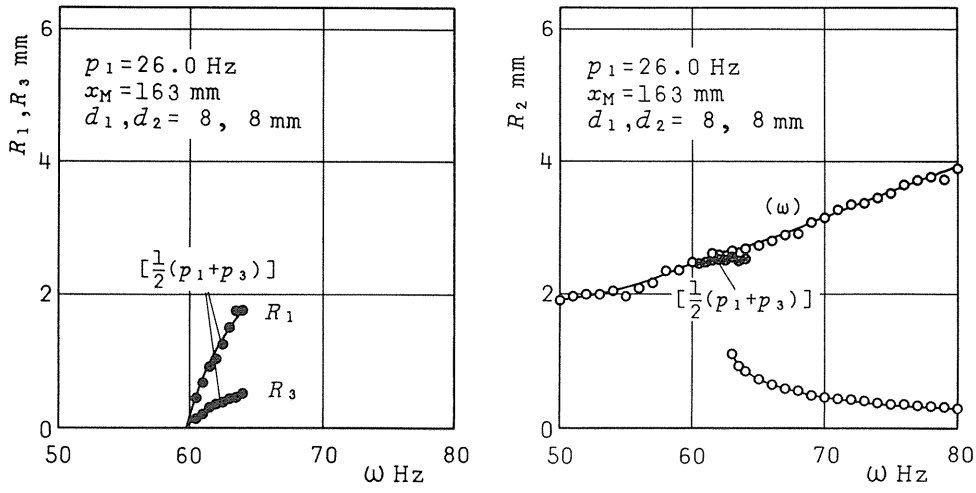

Fig. 2. 11. Response curves obtained experimentally near the second primary point (d_1=d_2).

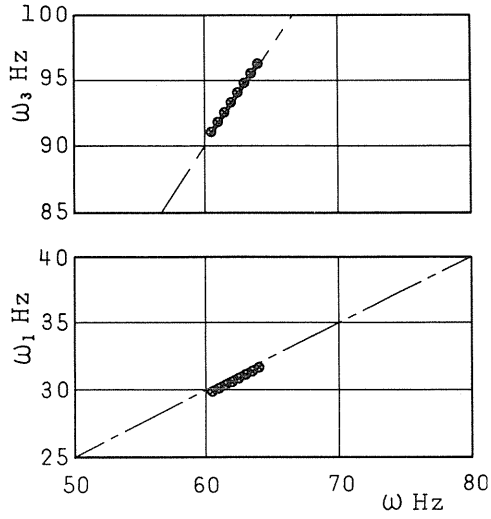

Fig. 2. 12. Frequencies of the components in the summed and differential harmonic oscillation.

$2\omega=\omega_1+\omega_3$. Thus, it was confirmed that the summed and differential harmonic oscillation occured.

The response curve obtained experimentally for the summed and differential harmonic oscillation is shown in Fig. 2. 11. In the figure, ○ denotes occurrence of the harmonic oscillation and ⊗ the occurrence of the summed and differential harmonic oscillation. The frequencies ω_1, ω_3 of the summed and differential harmonic oscillation obtained experimentally are shown in Fig. 2. 12. In the figure are added for comparison, chain lines expressing 1/2 times and 3/2 times the exciting frequency. These experimental results agree well with the results of the theoretical analysis.

2. 6. Oscillations near the third primary resonance point

2. 6. 1. Occurrence of subharmonic oscillations

The response near the third primary resonance point is obtained by putting $k=3$ in the analysis given in Sect. 2. 2. 3. For numerical analysis the first three modes are retained, and R_n, P_n and D_n ($n>3$) are neglected. Eq. (2.17) for this case is

$$
\left.\begin{aligned}
p_1R_1' &= -p_1\zeta R_1-\frac{3}{8}P_1R_1^2\sin 3\gamma_1-2(D_1P_2+D_2P_1)R_2\sin(\gamma_1+\gamma_2)\\
&\quad -2D_2R_2R_1\sin(2\gamma_1-\gamma_2)-\frac{1}{2}P_1R_2^2\sin(\gamma_1-2\gamma_2)\\
p_1R_1\gamma_1' &= \frac{1}{3}p_1\sigma R_1\\
&\quad -\{\sum_{m=1}^{3}m^2\left(\frac{1}{4}R_m^2+\frac{1}{4}P_m^2+\frac{1}{2}D_m^2\right)+\frac{1}{8}R_1^2+\frac{1}{2}P_1^2+D_1^2\}R_1\\
&\quad -\frac{3}{8}P_1R_1^2\cos 3\gamma_1-2(D_1P_2+D_2P_1)R_2\cos(\gamma_1+\gamma_2)\\
&\quad -2D_2R_2R_1\cos(2\gamma_1-\gamma_2)-\frac{1}{2}P_1R_2^2\cos(\gamma_1-2\gamma_2)\\
p_2R_2' &= -p_2\zeta R_2-2(D_1P_2+D_2P_1)R_1\sin(\gamma_2+\gamma_1)\\
&\quad -D_2R_1^2\sin(\gamma_2-2\gamma_1)-P_1R_1R_2\sin(2\gamma_2-\gamma_1)\\
p_2R_2\gamma_2' &= \frac{2}{3}p_2\sigma R_2\\
&\quad -4\{\sum_{m=1}^{3}m^2\left(\frac{1}{4}R_m^2+\frac{1}{4}P_m^2+\frac{1}{2}D_m^2\right)+\frac{4}{8}R_2^2+\frac{4}{2}P_2^2+4D_2^2\}R_2\\
&\quad -2(D_1P_2+D_2P_1)R_1\cos(\gamma_2+\gamma_1)\\
&\quad -D_2R_1^2\cos(\gamma_2-2\gamma_1)-P_1R_1R_2\cos(2\gamma_2-\gamma_1)\\
p_3R_3' &= -p_3\zeta R_3+\frac{1}{2}Q_{31}\sin\gamma_3\\
&\quad -\frac{9}{8}R_3\sum_{m=1}^{3}m^2P_m^2\sin 2\gamma_3-9D_3\sum_{m=1}^{3}m^2D_mP_m\sin\gamma_3
\end{aligned}\right\}\qquad(2.30)
$$

$$p_3 R_3 \gamma_3' = \frac{3}{3} p_3 \sigma R_3 + \frac{1}{2} Q_{31} \cos\gamma_3$$
$$-9\{\sum_{m=1}^{3} m^2 (\frac{1}{4} R_m^2 + \frac{1}{4} P_m^2 + \frac{1}{2} D_m^2) + \frac{9}{8} R_3^2 + \frac{9}{2} P_3^2 + 9 D_3^2\} R_3$$
$$-\frac{9}{8} R_3 \sum_{m=1}^{3} m^2 P_m^2 \cos 2\gamma_3 - 9 D_3 \sum_{m=1}^{3} m^2 D_m P_m \cos\gamma_3$$

The steady-state solutions of Eq. (2.30) can be classified into two groups, one with $R_1=R_2=0$ and the other with $R_1\neq 0$, $R_2\neq 0$. The former solutions imply occurrence of the harmonic oscillation, and the latter that of the oscillation containing subharmonic oscillations of orders 1/3 and 2/3. The latter oscillation will be called in this paper, with use of its components, the oscillation of type $(1/3\omega,\ 2/3\omega)$.

2. 6. 2. *Characteristics of subharmonic oscillations*

An example of the response curves obtained theoretically is shown in Fig. 2. 13. In the figures, R_3 denotes the amplitudes of the harmonic oscillations, and R_1 and R_2 denote the amplitudes of the subharmonic oscillations of orders 1/3 and 2/3, respectively.

As can be seen, the oscillations near the third primary resonance points can be classified into two types. To one belong the pure harmonic oscillations denoted by O_0 and O_2, and to the other belong the oscillations denoted by A and B which are accompanied with the subharmonic oscillations. Among the latter oscillations, the ones denoted by A are of type $(1/3\omega,\ 2/3\omega)$, with use of the notations employed in the previous section, because R_1 and R_2 are large enough. On the other hand, the oscillations denoted by B may be regarded as the usual subharmonic oscillations of order 1/3, because R_2 is small. Both the branches A and B are separated from the branches of the harmonic oscillations, so the oscillations denoted by A and B can occur only when appropriate initial conditions are given.

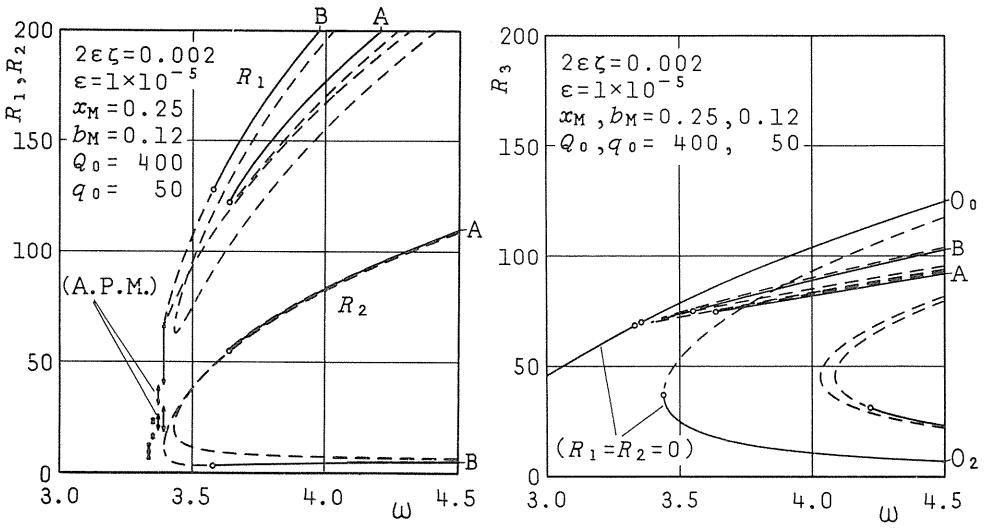

Fig. 2. 13. Response curves obtained theoretically near the third primary resonance point.

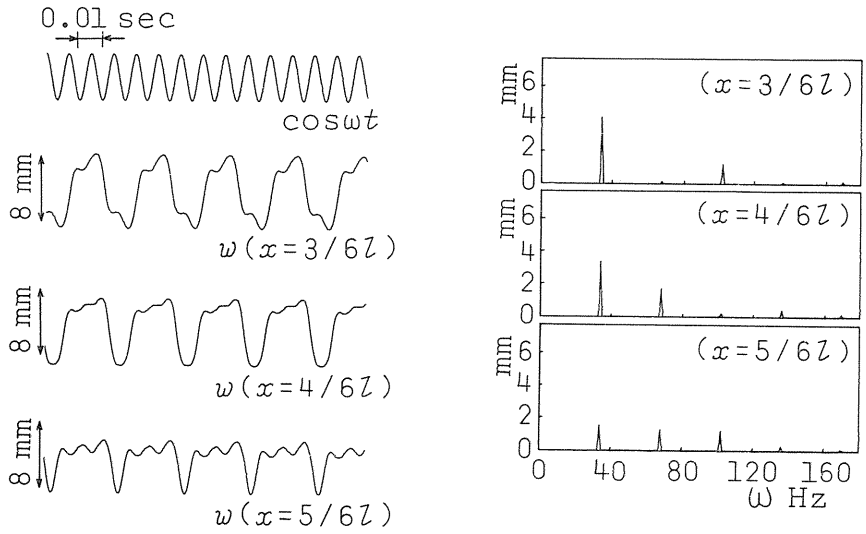

Fig. 2. 14. Waveform and spectrum of the oscillation of type (1/3ω, 2/3ω) near the third primary resonance point (102 Hz).

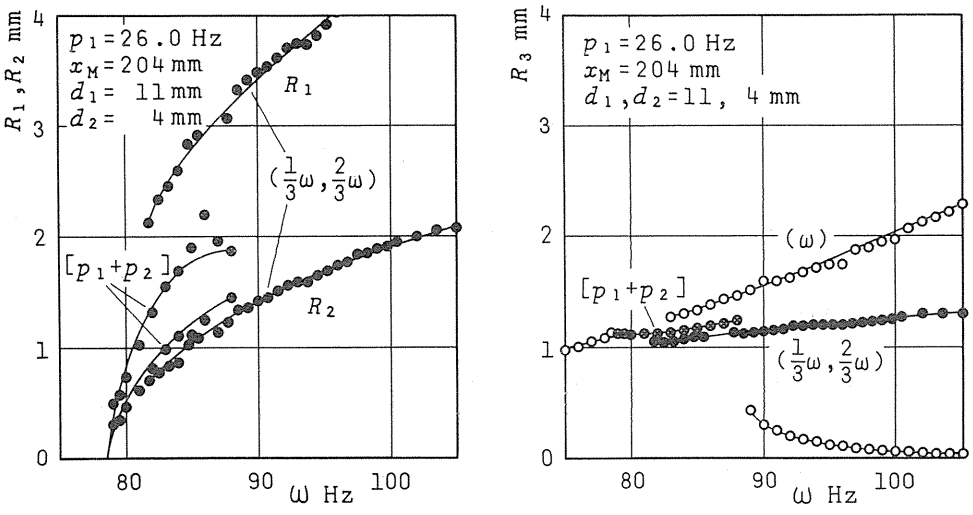

Fig. 2. 15. Response curves obtained experimentally near the third primary resonance point.

It is also found that an unstable portion exists on the branch O_0, and almost periodic motions occur in this portion. In Fig. 2. 13 is shown the range of variations of the amplitudes R_n of the almost periodic motions as segments with arrow heads. As the result of studies, these oscillations can be regarded as the so-called summed and differential harmonic oscillation.[21] These oscillations occur continuously only by varying the excitation frequency.

2. 6. 3. *Experimental results*

Near the third primary resonance point were observed the occurrences of such oscillations as shown in Fig. 2. 14. From the figures, it is seen that these oscillations are of type $(1/3\omega,\ 2/3\omega)$. The summed and differential harmonic oscillations were also observed. However the oscillation, predicted by the theory and regarded as a subharmonic oscillation of order 1/3, did not occur.

The response curves obtained experimentally are shown in Fig. 2. 15. In the figures, ○, ● and ⊗ denote the harmonic oscillations, the oscillations of type $(1/3\omega,\ 2/3\omega)$, and the summed and differential harmonic oscillation, respectively. The results confirm the validity of the theoretical analysis.

2. 7. *Oscillations near the fourth primary resonance point*

2. 7. 1. *Occurrence of subharmonic oscillations*

The response near the fourth primary resonance point is obtained by putting $k=4$ in the analysis given in Sect. 2. 2. 3. For numerical analysis, the first four modes are retained and R_n, P_n, and D_n $(n>4)$ are neglected. Eq. (2.17) for this case is

$$
\begin{aligned}
p_1R_1' &= -p_1\zeta R_1 - 2D_2R_2R_1\sin(2\gamma_1-\gamma_2) - P_2R_2R_1\sin(2\gamma_1+\gamma_2) \\
&\quad -\frac{9}{2}(D_1P_3+D_3P_1)R_3\sin(\gamma_1+\gamma_3) \\
p_1R_1\gamma_1' &= \frac{1}{4}p_1\sigma R_1 \\
&\quad -\{\sum_{m=1}^{4} m^2\left(\frac{1}{4}R_m^2+\frac{1}{4}P_m^2+\frac{1}{2}D_m^2\right)+\frac{1}{8}R_1^2+\frac{1}{2}P_1^2+D_1^2\}R_1 \\
&\quad -2D_2R_2R_1\cos(2\gamma_1-\gamma_2)-P_2R_2R_1\cos(2\gamma_1+\gamma_2) \\
&\quad -\frac{9}{2}(D_1P_3+D_3P_1)R_3\cos(\gamma_1+\gamma_3) \\
p_2R_2' &= -p_2\zeta R_2 - 4\left(\frac{1}{2}\sum_{m=1}^{4} m^2D_mP_m+4D_2P_2\right)R_2\sin 2\gamma_2 \\
&\quad -32D_4R_4R_2\sin(2\gamma_2-\gamma_4)-D_2R_1^2\sin(\gamma_2-2\gamma_1) \\
&\quad -\frac{1}{2}P_2R_1^2\sin(\gamma_2+2\gamma_1)-\frac{9}{2}P_2R_3^2\sin(\gamma_2-2\gamma_3)
\end{aligned}
$$

$$
\left.
\begin{aligned}
p_2R_2\gamma_2' &= \frac{2}{4}p_2\sigma R_2 \\
&\quad -4\{\sum_{m=1}^{4} m^2(\frac{1}{4}R_m^2+\frac{1}{4}P_m^2+\frac{1}{2}D_m^2)+\frac{4}{8}R_2^2+\frac{4}{2}P_2^2+4D_2^2\}R_2 \\
&\quad -4(\frac{1}{2}\sum_{m=1}^{4} m^2D_mP_m+4D_2P_2)R_2\cos 2\gamma_2 \\
&\quad -32D_4R_4R_2\cos(2\gamma_2-\gamma_4)-D_2R_1^2\cos(\gamma_2-2\gamma_1) \\
&\quad -\frac{1}{2}P_2R_1^2\cos(\gamma_2+2\gamma_1)-\frac{9}{2}P_2R_3^2\cos(\gamma_2-2\gamma_3) \\
p_3R_3' &= -p_3\zeta R_3-9P_2R_2R_3\sin(2\gamma_3-\gamma_2) \\
&\quad -\frac{9}{2}(D_1P_3+D_3P_1)R_3\sin(\gamma_3+\gamma_1) \\
p_3R_3\gamma_3' &= \frac{3}{4}p_3\sigma R_3 \\
&\quad -9\{\sum_{m=1}^{4} m^2(\frac{1}{4}R^2{}_m+\frac{1}{4}P^2{}_m+\frac{1}{2}D^2{}_m)+\frac{9}{8}R_3^2+\frac{9}{2}P_3^2+9D_3^2\}R_3 \\
&\quad -9P_2R_2R_3\cos(2\gamma_3-\gamma_2)-\frac{9}{2}(D_1P_3+D_3P_1)R_3\cos(\gamma_3+\gamma_1) \\
p_4R_4' &= -p_4\zeta R_4+\frac{1}{2}Q_{41}\sin\gamma_4-16D_4R_2^2\sin(\gamma_4-2\gamma_2) \\
&\quad -\frac{16}{8}R_4\sum_{m=1}^{4} m^2P_m^2\sin 2\gamma_4-16D_4\sum_{m=1}^{4} m^2D_mP_m\sin\gamma_4 \\
p_4R_4\gamma_4' &= \frac{4}{4}p_4\sigma R_4+\frac{1}{2}Q_{41}\cos\gamma_4-16D_4R_2^2\cos(\gamma_4-2\gamma_2) \\
&\quad -16\{\sum_{m=1}^{4} m^2(\frac{1}{4}R_m^2+\frac{1}{4}P_m^2+\frac{1}{2}D_m^2)+\frac{16}{8}R_4^2+\frac{16}{2}P_4^2+16D_4^2\}R_4 \\
&\quad -\frac{16}{8}R_4\sum_{m=1}^{4} m^2P_m^2\cos 2\gamma_4-16D_4\sum_{m=1}^{4} m^2D_mP_m\cos\gamma_4
\end{aligned}
\right\} \quad (2.31)
$$

The steady-state solutions of Eq. (2.31) can be classified into three groups, one with $R_1=R_2=R_3=0$ another with $R_1=R_3=0$, $R_2\neq 0$ and the other with $R_1\neq 0$, $R_3\neq 0$. The first solutions imply occurrence of the harmonic oscillation, the second imply occurrence of subharmonic oscillation of order 1/2 and the last that of the oscillation containing subharmonic oscillations of orders 1/4, 2/4 and 3/4. The latter oscillation will be called in this paper, with use of its components, the oscillation of type ($1/4\omega$, $2/4\omega$, $3/4\omega$).

2. 7. 2. Characteristics of subharmonic oscillations

An example of the response curves obtained theoretically is shown in Fig. 2. 16. In the figures, R_4 denotes the amplitudes of the harmonic oscillations, and R_1, R_2 and R_3 denote the amplitudes of the subharmonic oscillations of orders 1/4, 2/4 and 3/4, respectively.

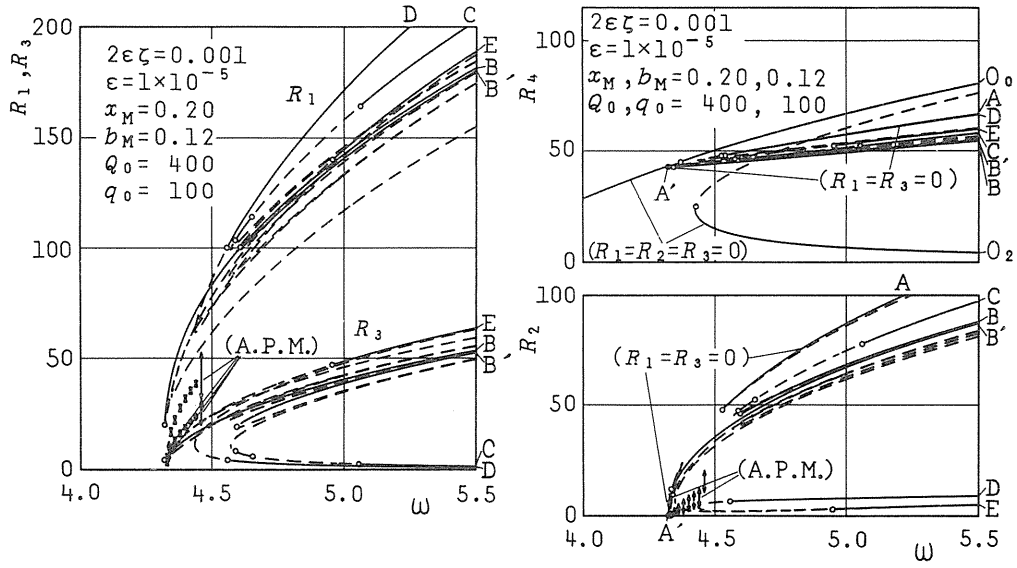

Fig. 2. 16. Response curves obtained theoretically near the fourth primary resonance point.

As can be seen, the oscillations near the fourth primary resonance point can be classified into three types. To the first belong oscillations denoted by O_0 and O_2, which are the harmonic oscillations with $R_1=R_2=R_3=0$. To the second belong oscillations denoted by A and A′, which are the subharmonic oscillations of order 1/2 with $R_1=R_3=0$. To the last belong the other types of subharmonic oscillations. Among the last, the oscillation denoted by B is an oscillation of type (1/4ω, 2/4ω, 3/4ω), because all components R_1, R_2 and R_3 are large enough. Also it is seen that unstable portions exist on branch A′ of the subharmonic oscillation of the order 1/2 as well as on branch O_0 of the harmonic oscillations. On each of these unstable portions occur almost periodic motions, among which the one occurring on the former portion can be regarded as the summed and differential harmonic oscillation.

As the branch A′ of the subharmonic oscillation of order 1/2 bifurcates from the branch O_0 of the harmonic oscillation, the subharmonic oscillation occurs continuously only by increasing the excitation frequency ω. When ω further increases, an almost periodic motion first occurs in the unstable portion of branch A′, and then an oscillation of type (1/4ω, 2/4ω, 3/4ω) of branch B occurs, both continuously.

2. 7. 3. *Experimental results*

Near the fourth primary resonance point were observed the occurrences of two types of oscillations as shown in Fig. 2. 17. From the figures it is seen that these are subharmonic oscillations of order 1/2 and oscillations of type (1/4ω, 2/4ω, 3/4ω). Other oscillations such as the summed and differential harmonic oscillations and almost periodic motions were also occurred experimentally.

The response curves obtained experimentally are shown in Fig. 2. 18. In the figures, ○, ●, ▲ and ⊗ denote the harmonic oscillations, the subharmonic oscillations of order 1/2, the oscillations of type (1/4ω, 2/4ω, 3/4ω), and the summed and differential harmonic

oscillations, respectively. The results of the experimental analysis confirm the validity of the theoretical analysis.

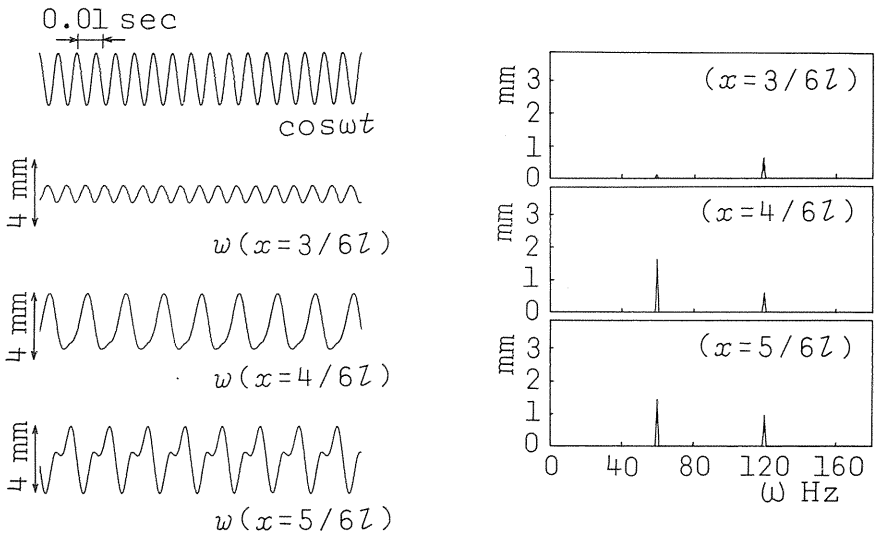

(a) Subharmonic oscillation of order 1/2 (120 Hz).

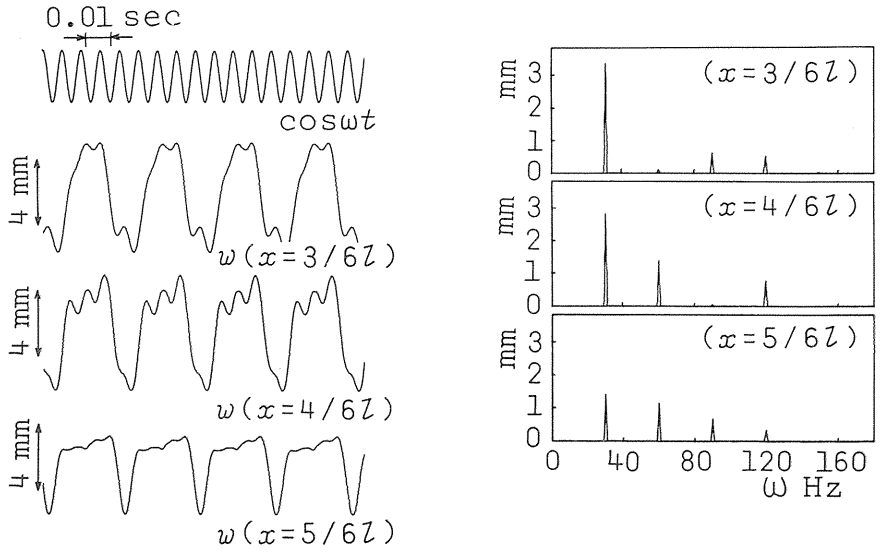

(b) Oscillation of type (1/4ω, 2/4ω, 3/4ω) (120 Hz).

Fig. 2. 17. Waveform and spectrum of oscillation near the fourth primary resonance point.

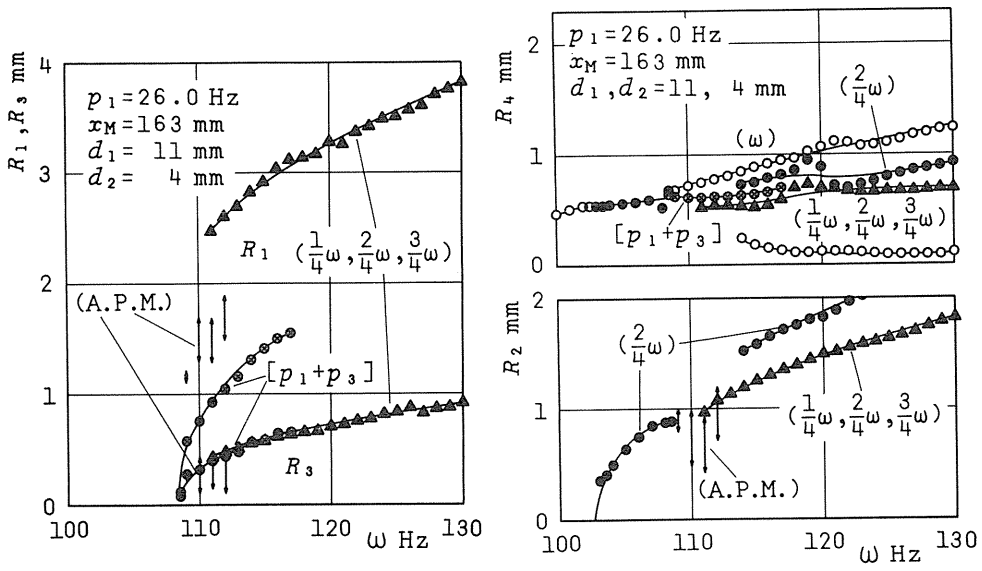

Fig. 2. 18. Response curves obtained experimentally near the fourth primary resonance point.

2. 8. *Conclusions*

The nonlinear oscillations near the first four primary resonance points of a string subjected to periodic excitation were treated theoretically and experimentally. The obtained results of the theoretical analysis are summarized as follows:

(1) Near the first primary resonance point, the oscillations containing the second and third super-harmonic oscillations can occur, in addition to the usual harmonic oscillation.

(2) Near the second primary resonance point, the subharmonic oscillations of order 1/2 and oscillations of type $(1/2\omega,\ 3/2\omega)$ can occur, when the external force contain a component independent of time. On the other hand, when the external force doesn't contain it or contain only slightly, the summed and differential harmonic oscillation occurs.

(3) Near the third primary resonance point, the subharmonic oscillations of order 1/3, the oscillations of type $(1/3\omega,\ 2/3\omega)$, and the summed and differential harmonic oscillations can occur in addition to the usual harmonic oscillation.

(4) Near the fourth primary resonance point, the subharmonic oscillation of order 1/2, the oscillations of type $(1/4\omega,\ 2/4\omega,\ 3/4\omega)$, the summed and differential harmonic oscillations, and almost periodic motions can occur in addition to the usual harmonic oscillation.

Thus it was shown theoretically that multi-mode response occurs in the string.

Finally, an experiment was conducted with use of a thin steel strip, and the validity of the theoretical analysis was confirmed.

3. Multi-mode Response of a Circular Membrane

3. 1. *Introduction*

Problems of nonlinear vibrations of a circular membrane have been treated by Eringen,[30] Chobotov and Binder,[31] Keller and Ting,[32] Mack and McQueary,[33]Yen and Lee,[34] the present authors,[25] and others. But almost all the investigations so far have been restricted to axisymmetric problems. Nonsymmetric problems have been hardly investigated.

In this chapter, a problem of nonlinear nonsymmetric vibrations of a circular membrane is taken up. The forced oscillations near a primary resonance point induced by harmonic nonsymmetric excitation is considered. It is known that in the nonsymmetric vibrational modes, two modes exist in pairs with the same natural frequency and with the same modal shape but are shifted circumferentially from each other by angle $\pi/2n$ (n is the number of nodal lines). In nonlinear problems, as will be shown later, these two modes are coupled by nonlinear terms. Hence it is expected that a multi-mode response can occur. Here it is shown that the multi-mode response in fact occurs.

For theoretical analysis, modal equations are first derived from the governing nonlinear partial differential equations. Then, a typical case is analyzed of forced oscillations near the primary resonance point at which the modes having one nodal line resonate. It will be shown that, near this primary resonance point, in addition to the usual harmonic oscillation, a special type oscillation occurs in which the modes in pairs are excited simultaneously with a phase lag of nearly $\pi/2$ between them, and a traveling wave occurs and moves circumferentially. Thus, it will be shown that the multi-mode response occurs in the form of traveling wave.

Finally, experimental analysis is conducted with use of a steel membrane to confirm the validity of the theoretical analysis.

3. 2. *Fundamental Equations and Modal Equations*

3. 2. 1. *Fundamental equations*

A circular membrane of radius a and thickness h, stretched by uniform tension N_0, and subjected to external force and damping force in the lateral direction, is considered. Polar coordinates (r,θ) is taken in the middle plane of the membrane in its equilibrium state, with the origin coinciding with the center of the membrane. As the inertia force, only the lateral component is retained. Under these assumptions, the equations of motion become as follows:

$$\left.\begin{aligned}
&\rho h\frac{\partial^2 w}{\partial t^2}+c\frac{\partial w}{\partial t}-N_0\nabla^2 w-q\\
&\quad=Nr\frac{\partial^2 w}{\partial r^2}+N_\theta\left(\frac{1}{r}\frac{\partial w}{\partial r}+\frac{1}{r^2}\frac{\partial^2 w}{\partial\theta^2}\right)-N_{r\theta}\left(\frac{2}{r^2}\frac{\partial w}{\partial\theta}-\frac{2}{r}\frac{\partial^2 w}{\partial r\partial\theta}\right)\\
&\frac{\partial N_r}{\partial r}+\frac{1}{r}\frac{\partial N_{r\theta}}{\partial\theta}+\frac{1}{r}(N_r-N_\theta)=0\\
&\frac{1}{r}\frac{\partial N_\theta}{\partial\theta}+\frac{\partial N_{r\theta}}{\partial r}+\frac{2}{r}N_{r\theta}=0
\end{aligned}\right\}\qquad(3.1)$$

In these equations, w and q are the deflection and the external force, respectively, both being functions of time as well as position. Also, ρ and c are the density of the membrane and the damping coefficient, respectively. Finally, N_r, N_θ, $N_{r\theta}$ are resultant forces in the membrane, and are related to deflection as well as radial and circumferential displacements u and v as follows:

$$\left.\begin{aligned} N_r &= \frac{Eh}{1-\nu^2}\left\{\frac{\partial u}{\partial r}+\frac{1}{2}\left(\frac{\partial w}{\partial r}\right)^2+\nu\frac{u}{r}+\frac{\nu}{r}\frac{\partial v}{\partial \theta}+\frac{\nu}{2}\left(\frac{1}{r}\frac{\partial w}{\partial \theta}\right)^2\right\} \\ N_\theta &= \frac{Eh}{1-\nu^2}\left\{\frac{u}{r}+\frac{1}{r}\frac{\partial v}{\partial \theta}+\frac{1}{2}\left(\frac{1}{r}\frac{\partial w}{\partial \theta}\right)^2+\nu\frac{\partial u}{\partial r}+\frac{\nu}{2}\left(\frac{\partial w}{\partial \theta}\right)^2\right\} \\ N_{r\theta} &= \frac{Eh}{2(1+\nu)}\left\{\frac{1}{r}\frac{\partial u}{\partial \theta}-\frac{v}{r}+\frac{\partial v}{\partial r}+\frac{1}{r}\frac{\partial w}{\partial r}\frac{\partial w}{\partial \theta}\right\} \end{aligned}\right\} \tag{3.2}$$

where, E and ν are Young's modulus and Poisson's ratio, respectively.

Suppose that N_r, N_θ, $N_{r\theta}$ are given in terms of stress function F in the form

$$\left.\begin{aligned} N_r &= \frac{1}{r}\frac{\partial F}{\partial r}+\frac{1}{r^2}\frac{\partial^2 F}{\partial \theta^2} \\ N_\theta &= \frac{\partial^2 F}{\partial r^2} \\ N_{r\theta} &= -\frac{\partial}{\partial r}\left(\frac{1}{r}\frac{\partial F}{\partial \theta}\right) \end{aligned}\right\} \tag{3.3}$$

With use of these expressions, the second and third of Eq. (3.1) are satisfied identically, while the first is rewritten as follows:

$$\rho h\frac{\partial^2 w}{\partial t^2}+c\frac{\partial w}{\partial t}-N_0\nabla^2 w=L(w,\ F)+q\ . \tag{3.4}$$

where

$$\begin{aligned} L(w,\ F)=&\left(\frac{1}{r}\frac{\partial F}{\partial r}+\frac{1}{r^2}\frac{\partial^2 F}{\partial \theta^2}\right)\frac{\partial^2 w}{\partial r^2}+\left(\frac{1}{r}\frac{\partial w}{\partial r}+\frac{1}{r^2}\frac{\partial^2 w}{\partial \theta^2}\right)\frac{\partial^2 F}{\partial r^2} \\ &-2\left(\frac{1}{r^2}\frac{\partial F}{\partial \theta}-\frac{1}{r}\frac{\partial^2 F}{\partial r\partial \theta}\right)\left(\frac{1}{r^2}\frac{\partial w}{\partial \theta}-\frac{1}{r}\frac{\partial^2 w}{\partial r\partial \theta}\right) \end{aligned} \tag{3.5}$$

Furthermore, the condition of compatibility of strains yields

$$\frac{1}{Eh}\nabla^4 F=-\frac{1}{2}L(w,\ w) \tag{3.6}$$

where $L(w,w)$ is an expression obtained from Eq. (3.5) by replacing F in its right hand side with w.

Introducing nondimensional quantities

$$\left.\begin{aligned} &\varepsilon=\frac{h}{a},\quad r'=\frac{r}{a},\quad t'=\frac{t}{a}\sqrt{\frac{N_0}{\rho h}},\quad w'=\frac{w}{a}\sqrt{\frac{Eh}{\varepsilon N_0}}\\ &F'=\frac{F}{\varepsilon N_0 a^2},\quad 2\varepsilon\zeta=\frac{ac}{\sqrt{\rho h N_0}},\quad \varepsilon q'=\frac{aq}{N_0}\sqrt{\frac{Eh}{\varepsilon N_0}} \end{aligned}\right\} \tag{3.7}$$

and rewriting Eqs. (3.4) and (3.6) in terms of these quantities, yields, after omitting primes, the following equations:

$$\left.\begin{aligned} &\frac{\partial^2 w}{\partial t^2}+2\varepsilon\zeta\frac{\partial w}{\partial t}-\nabla^2 w=\varepsilon L(w,\ F)+\varepsilon q\\ &\nabla^4 F=-\frac{1}{2}L(w,\ w) \end{aligned}\right\} \tag{3.8}$$

Boundary conditions are that u, v, and w are zero on the periphery of the membrane. Expressing these conditions in terms of w and F, by use of Eqs. (3.2), (3.3), yields

$$\left.\begin{aligned} &w|_{r=1}=0\\ &\{\frac{\partial^2 F}{\partial r^2}+\nu(\frac{1}{r}\frac{\partial F}{\partial r}+\frac{1}{r^2}\frac{\partial^2 F}{\partial\theta^2})\}|_{r=1}=0\\ &(\frac{1}{r^2}\frac{\partial F}{\partial\theta}-\frac{1}{r}\frac{\partial^2 F}{\partial r\partial\theta})|_{r=1}=0 \end{aligned}\right\} \tag{3.9}$$

3. 2. 2. Modal equations

To determine deflection w and stress function F in a form of series, the following two eigenvalue problems are solved in advance.

The first is the linear eigenvalue problem of a circular membrane. Namely, the problem is to solve the equation

$$\nabla^2 w=p^2 w \tag{3.10}$$

under the condition given by the first of Eq. (3.9). The eigenfunctions for the problem are, as is well known, as follows:

$$\{\Phi_{nn'}\cos n\,\theta,\ \Phi_{nn'}\sin n\,\theta\}\ \begin{pmatrix} n=0,1,\cdots\cdot\\ n'=1,2,\cdots\cdot\end{pmatrix} \tag{3.11}$$

where $\Phi_{nn'}$'s are given, with use of Bessel function of order n, as follows:

$$\Phi_{nn'}(r)=\varkappa_{nn'}J_n(p_{nn'}r) \tag{3.12}$$

In this expression, $p_{nn'}$'s are determined such that Eq. (3.12) satisfies the first of Eq. (3.9). In expressions (3.11), the two functions with the same suffixes nn' (where $n>1$) are modal forms of the modes, which have n nodal lines and $(n'-1)$ nodal circles but are shifted circumferentially from each other by angle $\pi/2n$. In the following, these modes and their natural frequency are denoted by the notation (n,n'). Arbitrary constants $k_{nn'}$ are assumed in the following to be determined by the normalization condition.

Another eigenvalue problem is to solve the equation

$$\nabla^4 F=\lambda^4 F \tag{3.13}$$

under the boundary conditions given by the second and third of Eq. (3.9). The eigenfunctions for this problem are

$$\{\Psi_{nn'}\cos n\,\theta,\ \Psi_{nn'}\sin n\,\theta\}\ \begin{pmatrix} n=0,1,\cdots\cdot \\ n'=1,2,\cdots\cdot \end{pmatrix} \tag{3.14}$$

where $\Psi_{nn'}$'s are given, with use of Bessel functions and modified Bessel functions of order n, as follows:

$$\Psi_{nn'}(r)=\mu_{nn'}\{J_n(\lambda_{nn'}r)+\chi_{nn'}I_n(\lambda_{nn'}r)\} \tag{3.15}$$

In these expressions, $\lambda_{nn'}$'s and $\chi_{nn'}$'s are determined such that Eq. (3.15) satisfies the boundary conditions. Here too, arbitrary constants are assumed to be determined by the normalization condition.

With use of the above two kinds of functions, w and F are developed in the following form:

$$\left.\begin{aligned} w&=\sum_{n=0}^{\infty}\sum_{n'=1}^{\infty}(X_{nn'}\cos n\theta+\widetilde{X}_{nn'}\sin n\theta)\Phi_{nn'} \\ F&=\sum_{n=0}^{\infty}\sum_{n'=1}^{\infty}(Y_{nn'}\cos n\theta+\widetilde{Y}_{nn'}\sin n\theta)\Psi_{nn'} \end{aligned}\right\} \tag{3.16}$$

where $X_{nn'}$, $\widetilde{X}_{nn'}$, and $Y_{nn'}$, $\widetilde{Y}_{nn'}$ are unknown functions of time to be determined. Among them, $X_{nn'}$ and $\widetilde{X}_{nn'}$ denote the magnitudes of modes of order (n,n') contained in the deflection.

To obtain equations for determining $X_{nn'}$, $\widetilde{X}_{nn'}$ and $Y_{nn'}$, $\widetilde{Y}_{nn'}$, Eq. (3.16) is substituted into Eq. (3.8). Then, in the resulting equations, the first and second are multiplied by $r\Phi_{nn'}\cos n\theta$, $r\Phi_{nn'}\sin n\theta$ and $r\Psi_{nn'}\cos n\theta$, $r\Psi_{nn'}\sin n\theta$, respectively, and each is integrated in the region of the membrane. Due to the orthogonality of the eigenfunctions, this yields the following equations:

$$\left.\begin{aligned} &\ddot{X}_{nn'}+2\varepsilon\zeta\dot{X}_{nn'}+p^2{}_{nn'}X_{nn'}-\varepsilon Q_{nn'} \\ &\quad=\varepsilon\sum_{m,i=0}^{\infty}\sum_{m',i'=1}^{\infty}(a_{nn'mm'ii'}Y_{mm'}X_{ii'}+b_{nn'mm'ii'}\widetilde{Y}_{mm'}\widetilde{X}_{ii'}) \\ &\ddot{\widetilde{X}}_{nn'}+2\varepsilon\zeta\dot{\widetilde{X}}_{nn'}+p^2{}_{nn'}\widetilde{X}_{nn'}-\varepsilon\widetilde{Q}_{nn'} \\ &\quad=\varepsilon\sum_{m,i=0}^{\infty}\sum_{m',i'=1}^{\infty}(c_{nn'mm'ii'}Y_{mm'}\widetilde{X}_{ii'}+d_{nn'mm'ii'}\widetilde{Y}_{mm'}X_{ii'}) \end{aligned}\right\} \tag{3.17}$$

$$\left.\begin{aligned} Y_{mm'} &= \sum_{j,k=0}^{\infty} \sum_{j',k'=1}^{\infty} (\alpha_{mm'jj'kk'} X_{jj'} X_{kk'} + \beta_{mm'jj'kk'} \tilde{X}_{jj'} \tilde{X}_{kk'}) \\ \tilde{Y}_{mm'} &= \sum_{j,k=0}^{\infty} \sum_{j',k'=1}^{\infty} (\gamma_{mm'jj'kk'} X_{jj'} \tilde{X}_{kk'} + \delta_{mm'jj'kk'} \tilde{X}_{jj'} X_{kk'}) \end{aligned}\right\}$$

Finally, of these equations the third and fourth are substituted into the first and second to yield the required modal equations in the form

$$\left.\begin{aligned} &\ddot{X}_{nn'} + 2\varepsilon\zeta\dot{X}_{nn'} + p^2_{nn'} X_{nn'} - \varepsilon Q_{nn'} \\ &\quad = \varepsilon \sum_{i,j,k=0}^{\infty} \sum_{i',j',k'=1}^{\infty} (A_{nn'ii'jj'kk'} X_{ii'} X_{jj'} X_{kk'} + B_{nn'ii'jj'kk'} X_{ii'} \tilde{X}_{jj'} \tilde{X}_{kk'} \\ &\qquad + C_{nn'ii'jj'kk'} \tilde{X}_{ii'} X_{jj'} \tilde{X}_{kk'} + D_{nn'ii'jj'kk'} \tilde{X}_{ii'} \tilde{X}_{jj'} X_{kk'}) \\ &\ddot{\tilde{X}}_{nn'} + 2\varepsilon\zeta\dot{\tilde{X}}_{nn'} + p^2_{nn'} \tilde{X}_{nn'} - \varepsilon \tilde{Q}_{nn'} \\ &\quad = \varepsilon \sum_{i,j,k=0}^{\infty} \sum_{i',j',k'=1}^{\infty} (\tilde{A}_{nn'ii'jj'kk'} \tilde{X}_{ii'} \tilde{X}_{jj'} \tilde{X}_{kk'} + \tilde{B}_{nn'ii'jj'kk'} \tilde{X}_{ii'} X_{jj'} X_{kk'} \\ &\qquad + \tilde{C}_{nn'ii'jj'kk'} X_{ii'} \tilde{X}_{jj'} X_{kk'} + \tilde{D}_{nn'ii'jj'kk'} X_{ii'} X_{jj'} \tilde{X}_{kk'}) \end{aligned}\right\} \quad (3.18)$$

Here dot means differentiation with respect to time. As seen in these equations, the equations for determining X_{nn} and $\tilde{X}_{nn}$ are coupled by nonlinear terms.

3. 3. Oscillations near the Primary Resonance Point

3. 3. 1. Analysis by the perturbation method

By use of the modal equations derived in Sect. 3. 2. 2, the dynamic response of a membrane subjected to arbitrary excitation can be analyzed. Here the case in which the excitation is a harmonic function of the form $q=q(r,\theta)\cos\omega t$, and its frequency is near one of the natural frequencies, is taken up.

As a numerical example, it is assumed that $q(r,\theta)$ is symmetric with respect to θ. For such $q(r,\theta)$, it follows that $\tilde{Q}_{nn'}=0$ as to the components of the excitation. Also, it is assumed that ω is close to the natural frequency of order (1,1).

The concrete distribution of the excitation is taken so that it approximates the distribution in the experiment, which will be mentioned later. Namely, $q(r,\theta)$ takes the constant value q_0 inside, and zero outside, of the circular region of radius r_0 with center $(r,\theta)=(r_M,0)$.

To carry out numerical calculation, equations with $n=1$, $n'=1$ in Eq. (3.18) are retained, and the unknown quantities other than X_{11}, $\tilde{X}_{11}$ are neglected. Thus, the equations to be solved are

$$\left.\begin{aligned} &\ddot{X} + 2\varepsilon\zeta\dot{X} + p^2 X = \varepsilon A (X^2 + \tilde{X}^2) X + \varepsilon Q \cos\omega t \\ &\ddot{\tilde{X}} + 2\varepsilon\zeta\dot{\tilde{X}} + p^2 \tilde{X} = \varepsilon A (X^2 + \tilde{X}^2) \tilde{X} \end{aligned}\right\} \quad (3.19)$$

where

$$\left.\begin{aligned} &X=X_{11},\ \widetilde{X}=\widetilde{X}_{11},\ p=p_{11},\ Q\cos\omega t=Q_{11}\\ &A=A_{11111111}=B_{11111111}+C_{11111111}+D_{11111111}\\ &\quad=\widetilde{A}_{11111111}=\widetilde{B}_{11111111}+\widetilde{C}_{11111111}+\widetilde{D}_{11111111} \end{aligned}\right\} \tag{3.20}$$

To solve Eq. (3.19), it is assumed that the detuning between the excitation frequency ω and the natural frequency p is a small quantity of the order of ε so that ω can be put in the form

$$\omega=p+\varepsilon\sigma \tag{3.21}$$

As a method for solving the problem, the perturbation method of multiple scales[4] will be adopted. For this purpose, the solution is put in the form

$$\left.\begin{aligned} &X=X_0(T_0,T_1,\cdots\cdots)+\varepsilon X_1(T_0,T_1,\cdots\cdots)+\cdots\cdots\\ &\widetilde{X}=\widetilde{X}_0(T_0,T_1,\cdots\cdots)+\varepsilon\widetilde{X}_1(T_0,T_1,\cdots\cdots)+\cdots\cdots \end{aligned}\right\} \tag{3.22}$$

where $T_0=t$, $T_1=\varepsilon t$,... are times of different scales.

Now, to obtain the solutions within an accuracy of order ε, Eq. (3.19) is solved in the form

$$\left.\begin{aligned} &X_0=Ce^{i\sigma T_1}+\overline{C}e^{-i\sigma T_1}\\ &\widetilde{X}_0=De^{i\sigma T_1}+\overline{D}e^{-i\sigma T_1} \end{aligned}\right\} \tag{3.23}$$

Here, C and D are unknown functions of T_1, and $\overline{C}$ and $\overline{D}$ are their conjugates. These unknown quantities are determined from the condition that the solution has no secular terms, namely

$$\left.\begin{aligned} &2ipC'+2ip\zeta C-\frac{1}{2}Qe^{i\sigma T_1}\\ &\quad-A(3C^2\overline{C}+2D\overline{D}C+D^2\overline{C})=0\\ &2ipD'+2ip\zeta D\\ &\quad-A(3D^2\overline{D}+2C\overline{C}D+C^2\overline{D})=0 \end{aligned}\right\} \tag{3.24}$$

where primes mean differentiation with respect to T_1.

To solve Eq. (3.24), C and D are put in the form

$$\left.\begin{aligned} &C=\frac{1}{2}Re^{i(\sigma T_1-\gamma)}\\ &D=\frac{1}{2}\widetilde{R}e^{i(\sigma T_1-\widetilde{\gamma})} \end{aligned}\right\} \tag{3.25}$$

Substituting these expressions into Eq. (3.24) and dividing the resulting equations into real and imaginary parts, yields

$$\left.\begin{aligned} pR' &= -p\zeta R+\frac{1}{2}Q\sin\gamma+\frac{1}{8}A\widetilde{R}^2 R\sin(2\gamma-2\widetilde{\gamma}) \\ pR\gamma' &= p\sigma R+\frac{1}{2}Q\cos\gamma+\frac{3}{8}AR^3 \\ &\quad +\frac{1}{8}A\widetilde{R}^2 R\{2+\cos(2\gamma-2\widetilde{\gamma})\} \\ p\widetilde{R}' &= -p\zeta\widetilde{R}+\frac{1}{8}AR^2\widetilde{R}\sin(2\widetilde{\gamma}-2\gamma) \\ p\widetilde{R}\widetilde{\gamma}' &= p\sigma\widetilde{R}+\frac{3}{8}A\widetilde{R}^3+\frac{1}{8}AR^2\widetilde{R}\{2+\cos(2\widetilde{\gamma}-2\gamma)\} \end{aligned}\right\} \qquad (3.26)$$

To obtain a steady-state solution of the above equations, R', $\widetilde{R}'$, γ', $\widetilde{\gamma}'$ in them are put as zero. Solving the resulting equations and substituting the obtained solutions into Eqs. (3.25), (3.23), and then into (3.16), yields a solution of Eq. (3.8) in the following form:

$$w=R\cos(\omega t-\gamma)\Phi_{11}(r)\cos n\,\theta+\widetilde{R}\cos(\omega t-\widetilde{\gamma})\Phi_{11}(r)\sin n\,\theta \qquad (3.27)$$

From Eq. (3.26) it is seen that there are two kinds of steady-state solutions. One is a solution with $\widetilde{R}=0$. Noting that $\widetilde{Q}=0$ this solution expresses the occurrence of the usual harmonic oscillation. The other is a solution with $\widetilde{R}\neq 0$. This means that the two modes in pairs with the same natural frequency are induced simultaneously due to nonlinear coupling.

The stability of a steady-state solution (which is denoted by C, D) of Eq. (3.24) can be determined by giving to it a small disturbance (which is denoted by ΔC, ΔD) and examining its variation with respect to time. To examine this, C, D in Eq. (3.24) are replaced by $C+\Delta C$, $D+\Delta D$. Then, in the resulting equations, small quantities higher than the second order are neglected to obtain differential equations governing ΔC and ΔD. To rewrite the last equations in the form having real coefficients, ΔC and ΔD in them are put in the form

$$\left.\begin{aligned} \Delta C &= \frac{1}{2}(\xi+i\eta)e^{i\sigma T_1} \\ \Delta D &= \frac{1}{2}(\widetilde{\xi}+i\widetilde{\eta})e^{i\sigma T_1} \end{aligned}\right\} \qquad (3.28)$$

and substituted, and the resulting equations are divided into real and imaginary parts. Obtaining the eigenvalues of the final equations and examining the sign of their real parts determines the stability.

3. 3. 2. Characteristics of the oscillations

Characteristics of the oscillations are now examined via a numerical example. The

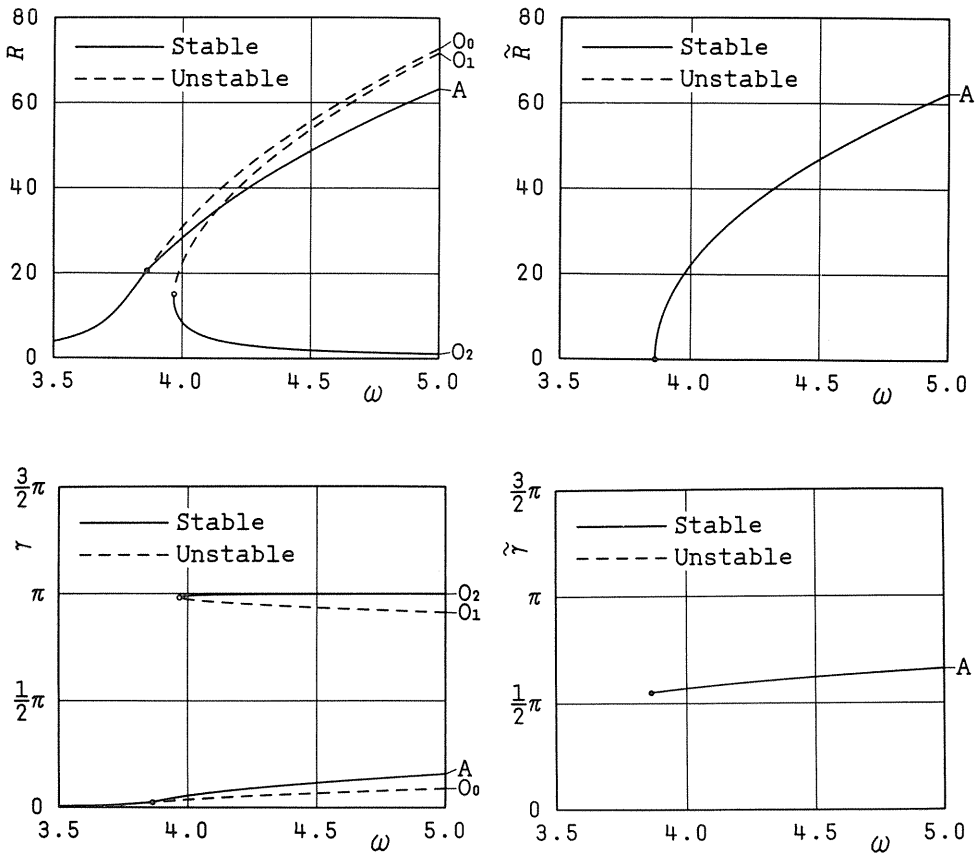

(ν=0.3, $2\varepsilon\zeta$=0.01, ε=1×10^{-3}, q_0=50, r_M=0.5, r_0=0.25)

Fig. 3. 1. Response and phase curves obtained theoretically.

response and phase curves in the example are shown in Fig. 3. 1. In the figures, solid and dotted lines denote stable and unstable oscillations, respectively. It is seen in the figures that the response curve consists of branches O_0, O_1, O_2 with $\widetilde{R}\neq 0$ as well as branch A with $\widetilde{R}\neq 0$. Branch A bifurcates from branch O_0, and the bifurcating point (denoted by ● in the figure) coincides with the boundary point between stable and unstable portions.

From the figures, the characteristics of the oscillations can be seen. When, for example, ω increases gradually from a lower value, the harmonic oscillation denoted by branch O_0 appears first. Then, when ω exceeds the value of ● the transition occurs from the harmonic oscillation to the oscillation denoted by branch A, and the latter oscillation consists of the components which take the shapes of the modes in pairs of order (1,1). When ω becomes sufficiently large in the last vibratory state, R and $\widetilde{R}$ take almost the same value. (Both approach gradually $\sqrt{3}/2$ times the value given by the backbone curve). And the phase difference between the two components is $\pi/2$, as obtained by comparing γ and $\widetilde{\gamma}$. Thus, in the last vibratory state, a traveling wave occurs with the angular speed equal to the excitation frequency, as seen from Eq. (3.27).

3. 4. *Experimental Analysis*

3. 4. 1. *Experimental method*

To confirm the validity of the theoretical analysis, an experimental analysis is conducted with use of a steel membrane. Schematic diagram of the experimental apparatus is given in Fig. 3. 2. In this apparatus, the ring shown in the figures is used to given tension to the membrane. Harmonic excitation is given by use of two electromagnets M_1 and M_2. Two displacement sensors are placed at angles π and $\pi/2$ measured from the position of the electromagnets so that the variation of X and $\widetilde{X}$ can be obtained independently of each other. The electromagnets are placed such that its midpoint coincides with point $(0.5a,0)$.

The dimensions and physical properties of the membrane used in the experiment are as follows:

radius	$a=215$ mm
thickness	$h=0.17$ mm
Young's modulus	$E=206$ GPa
Poisson's ratio	$\nu=0.3$
density	$\rho=7.7\times10^3$ Kg/m^3

The natural frequency p_{11} was obtained as $p_{11}/2\pi=150$ Hz

3. 4. 2. *Experimental results*

In the membrane excited by the excitation with a frequency close to the natural frequency of order (1,1), an oscillation as shown in the left side in Fig. 3. 3 was observed. In this figure, the upper and lower figures show the oscillatory waves at positions $\theta=\pi$ and $\theta=\pi/2$, respectively. These two waves show variation of X and $\widetilde{X}$ appearing in Eq.

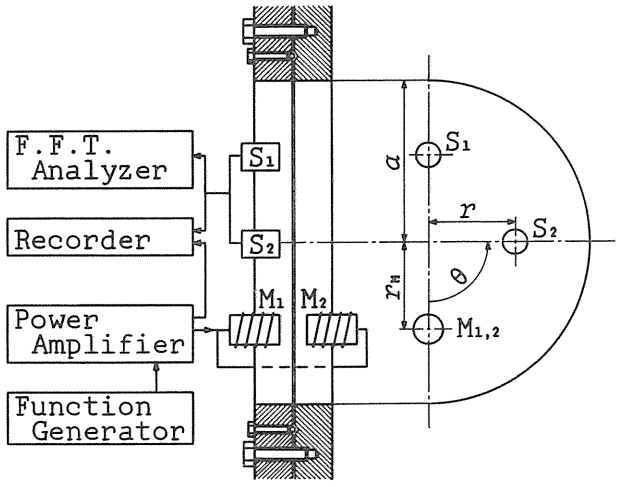

Fig. 3. 2. Schematic diagram of the experimental apparatus.

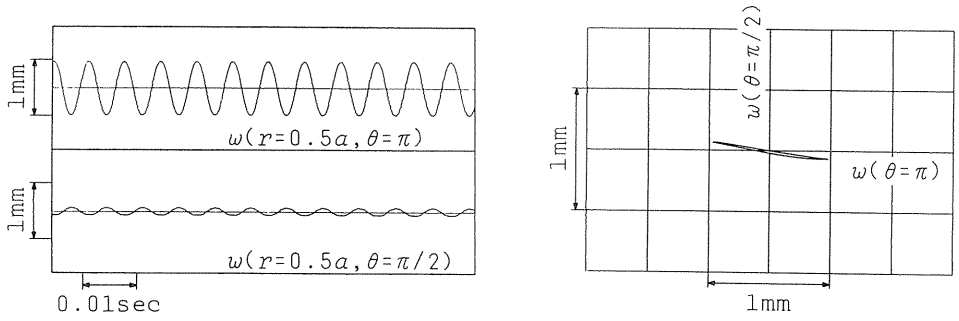

(a) 150 Hz

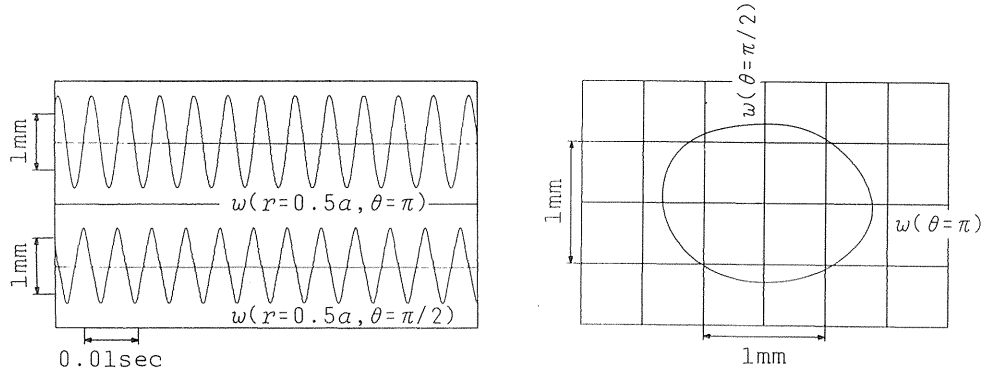

(b) 158 Hz

Fig. 3. 3. Waveform and Lissajous' figure.

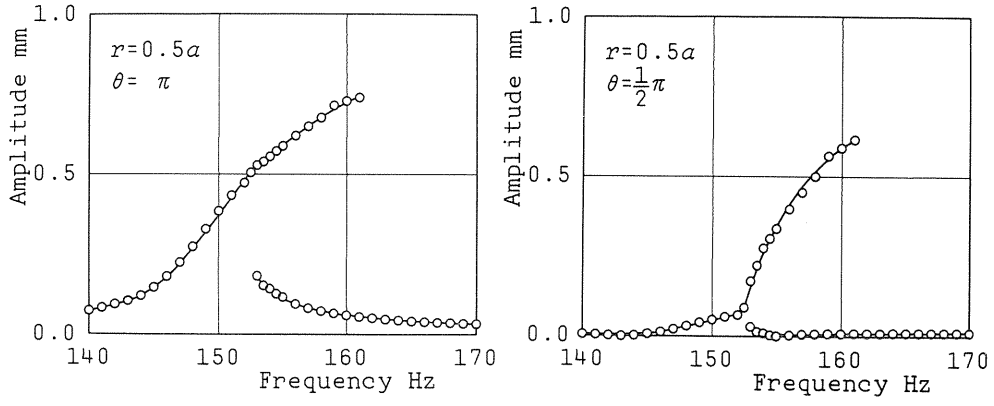

Fig. 3. 4. Response curves obtained experimentally.

(3.16). In the right side in Fig. 3. 3 are given Lissajous' figures obtained when values of the upper and lower waves are taken as abscissa and ordinate. In Fig. 3. 4 is given the response curve obtained experimentally. As in Fig. 3. 3, the amplitudes at the positions $\theta=\pi$ and $\theta=\pi/2$ correspond R and $\widetilde{R}$ in Eq. (3.27), and hence the response curve in Fig. 3. 4 corresponds to that of Fig. 3. 1.

From Figs. 3. 3 and 3. 4, the following can be said as to the characteristics of the oscillation. When ω is small, $\widetilde{R}$ is nearly zero, but when ω exceeds a certain value, $\widetilde{R}$ begins to increase rapidly. And when $\widetilde{R}$ is large enough, the phase difference between the oscillations with the amplitudes R and $\widetilde{R}$ is nearly $\pi/2$, as seen from the waves or Lissajous' figures in Fig. 3. 3. Thus, when ω is small the usual harmonic oscillation occurs, but when ω exceeds a certain value, a motion represented by branch A in Fig. 3. 1 occurs.

The above results agree qualitatively well with the theoretical results.

3. 5. Conclusions

As a problem of nonlinear nonsymmetric oscillations of a circular membrane, forced oscillations near a primary resonance point induced by a harmonic excitation are considered. As a typical example, an oscillation induced near the primary resonance point of order (1,1) is analyzed. The obtained results can be summarized as follows:

(1) First, the modal equations are derived from the governing partial differential equations.

(2) In the modal equations, the modes in pairs having the same natural frequency are coupled by nonlinear terms.

(3) Due to the above coupling, the modes in pairs can be excited simultaneously.

(4) When the modes in pairs are excited simultaneously, the phase difference between these modes is nearly $\pi/2$. Thus, a traveling wave can occur moving circumferentially with an angular speed equal to the excitation frequency. Hence, the multi-mode response occurs in the form of traveling wave.

Finally, experimental analysis is conducted with use of a steel membrane, and it is verified that the theoretical analysis is reasonable.

4. Multi-mode Response of a Square Membrane

4. 1. Introduction

The problems of nonlinear oscillations of a membrane have been the subjects of many investigators.[30–36] But the investigations concerning to forced oscillations are few. Especially those of the multi-mode responses which are often observed in the membrane, have scarcely been investigated.

In the previous chapter, the problem of forced oscillations of a circular membrane is considered. Then it was shown that a multi-mode response can occur, and that the two modes in a multi-mode response occur in such a way that they form a rotary type of oscillation.

In this chapter the problem of forced oscillations of a square membrane is taken up. It is known that in a square membrane, two modes exist in pairs with the same natural frequency and with the same modal shape. Due to this, the oscillations similar to those in circular membrane, and different from those in a rectangular membrane[37] are expected to occur.

For theoretical analysis, modal equations are first derived from the Karman-type equations which govern the motion of the square membrane. Then by taking up a typical case, the characteristics of oscillations of a square membrane subjected to harmonic excitation are discussed. The typical case taken up here is the one in which the excitation frequency comes near the resonance point of the modes with one nodal line. It will be shown by the analysis that in the square membrane a rotary type of oscillation as well as another type of oscillation which has no counterpart in a circular membrane occurs.

Lastly an experimental analysis is conducted with use of a thin steel membrane and the validity of the theoretical analysis is discussed.

4. 2. Fundamental Equations

4. 2. 1. Equations of motion of a membrane

Let a membrane with its side length a and thickness h, stretched by uniform tension N_0, be subjected to lateral excitation force and lateral viscous damping force. To express the equations of motion of the membrane, a rectangular coordinate O-xy is taken along two neighboring sides in the middle plane of the membrane in its equilibrium state. Then the Karman-type equations of motion is as follows:

$$\left.\begin{aligned} &\rho h\frac{\partial^2 w}{\partial t^2}+c\frac{\partial w}{\partial t}-N_0\nabla^2 w-q \\ &\quad=\frac{\partial^2 F}{\partial y^2}\cdot\frac{\partial^2 w}{\partial x^2}-2\frac{\partial^2 F}{\partial x\,\partial y}\cdot\frac{\partial^2 w}{\partial x\,\partial y}+\frac{\partial^2 F}{\partial x^2}\cdot\frac{\partial^2 w}{\partial y^2} \\ &\nabla^4 F=\frac{1}{Eh}\left\{\left(\frac{\partial^2 w}{\partial x\,\partial y}\right)^2-\frac{\partial^2 w}{\partial x^2}\cdot\frac{\partial^2 w}{\partial y^2}\right\} \end{aligned}\right\} \tag{4.1}$$

where w, F and q are deflection of the membrane, stress function determinig the membrane force, and the excitation force, all being functions of the coordinates x, y as well as time t. The quantities ρ, E and c are density, Young's modulus and damping coefficient, respectively. Also

$$\nabla^2=\frac{\partial^2}{\partial x^2}+\frac{\partial^2}{\partial y^2},\quad \nabla^4=\frac{\partial^4}{\partial x^4}+2\frac{\partial^4}{\partial x^2\,\partial y^2}+\frac{\partial^4}{\partial y^4} \tag{4.2}$$

By denoting the displacements in x and y directions by u and v, the relations between stress and strain are given as follows:

$$\left.\begin{aligned} &Eh\left\{\frac{\partial u}{\partial x}+\frac{1}{2}\left(\frac{\partial w}{\partial x}\right)^2\right\}=\frac{\partial^2 F}{\partial y^2}-\nu\frac{\partial^2 F}{\partial x^2} \\ &Eh\left\{\frac{\partial v}{\partial y}+\frac{1}{2}\left(\frac{\partial w}{\partial y}\right)^2\right\}=\frac{\partial^2 F}{\partial x^2}-\nu\frac{\partial^2 F}{\partial y^2} \\ &Eh\left\{\frac{\partial u}{\partial y}+\frac{\partial v}{\partial x}+\frac{\partial w}{\partial x}\cdot\frac{\partial w}{\partial y}\right\}=-2(1+\nu)\frac{\partial^2 F}{\partial x\,\partial y} \end{aligned}\right\} \tag{4.3}$$

where ν is Poisson's ratio.

Introducing the nondimensional quantities

$$\left.\begin{aligned}
&\varepsilon=\frac{h}{a},\ x'=\frac{x}{a},\ y'=\frac{y}{a},\ t'=\frac{t}{a}\sqrt{\frac{N_0}{\rho h}},\ w'=\pi^2\frac{w}{a}\sqrt{\frac{Eh}{\varepsilon N_0}}\\
&u'=\pi^2\frac{u}{a}\cdot\frac{Eh}{\varepsilon N_0},\ v'=\pi^2\frac{v}{a}\cdot\frac{Eh}{\varepsilon N_0},\ F'=\pi^2\frac{F}{\varepsilon N_0 a^2}\\
&2\varepsilon\zeta=\frac{ac}{\pi\sqrt{\rho h N_0}},\ \varepsilon q'=\frac{aq}{\pi N_0}\sqrt{\frac{Eh}{\varepsilon N_0}}
\end{aligned}\right\} \tag{4.4}$$

into Eq. (4.1) and omitting primes yields:

$$\left.\begin{aligned}
&\frac{\partial^2 w}{\partial t^2}+2\varepsilon\zeta\frac{\partial w}{\partial t}-\frac{1}{\pi^2}\nabla^2 w-\varepsilon q\\
&\quad=\frac{\varepsilon}{\pi^4}\left\{\frac{\partial^2 F}{\partial y^2}\cdot\frac{\partial^2 w}{\partial x^2}-2\frac{\partial^2 F}{\partial x\,\partial y}\cdot\frac{\partial^2 w}{\partial x\,\partial y}+\frac{\partial^2 F}{\partial x^2}\cdot\frac{\partial^2 w}{\partial y^2}\right\}\\
&\nabla^4 F=\left(\frac{\partial^2 w}{\partial x\,\partial y}\right)^2-\frac{\partial^2 w}{\partial x^2}\cdot\frac{\partial^2 w}{\partial y^2}
\end{aligned}\right\} \tag{4.5}$$

The boundary conditions on the four sides (x=0,1, y=0,1) are

$$w=0,\ u=0,\ v=0 \tag{4.6}$$

It is cumbersome to obtain the solutions which satisfy all the boundary conditions exactly. Instead it is tried here, as done in 38) and 39), to obtain such solutions that satisfy the first of the boundary conditions exactly, but the rest conditions only in the average. For this purpose the last two conditions are replaced by

$$\left.\begin{aligned}
&\int_0^1\int_0^1\left(\frac{\partial u}{\partial x}\right)dx\,dy=0\\
&\int_0^1\int_0^1\left(\frac{\partial v}{\partial y}\right)dx\,dy=0\\
&\int_0^1\int_0^1\left(\frac{\partial u}{\partial y}+\frac{\partial v}{\partial x}\right)dx\,dy=0
\end{aligned}\right\} \tag{4.7}$$

Substituting the nondimensional quantities given in Eq. (4.3) into Eq. (4.7) yields

$$\left.\begin{aligned}
&\int_0^1\int_0^1\left\{\frac{\partial^2 F}{\partial y^2}-\nu\frac{\partial^2 F}{\partial x^2}-\frac{1}{2}\left(\frac{\partial w}{\partial x}\right)^2\right\}dx\,dy=0\\
&\int_0^1\int_0^1\left\{\frac{\partial^2 F}{\partial x^2}-\nu\frac{\partial^2 F}{\partial y^2}-\frac{1}{2}\left(\frac{\partial w}{\partial y}\right)^2\right\}dx\,dy=0\\
&\int_0^1\int_0^1\left\{2(1+\nu)\frac{\partial^2 F}{\partial x\,\partial y}+\frac{\partial w}{\partial x}\cdot\frac{\partial w}{\partial y}\right\}dx\,dy=0
\end{aligned}\right\} \tag{4.8}$$

4. 2. 2. Modal equations

To obtain the unknown quantity w in the form of the superposition of the modes of a linearized system, it is noted first that the mode shape is given as follows:

$$w_{mn}=\sin m\,\pi\,x\,\sin n\,\pi\,y\quad(m,n=1,2,\cdots) \tag{4.9}$$

This mode shape is referred in what follows to that of order (m,n). Now w is sought in the form:

$$w=\sum_{m,n=1}^{\infty}X_{mn}\sin m\,\pi\,x\,\sin n\,\pi\,y \tag{4.10}$$

Here X_{mn}'s are unknown functions of time and express the magnitude of the mode of order (m,n) contained in w. This expression satisfies the first of the boundary conditions exactly.

Another unknown quantity F is supposed to be given in the following form:

$$F=\sum_{m,n=1}^{\infty}Y_{mn}\sin m\,\pi\,x\,\sin n\,\pi\,y+\frac{1}{2}N_{x0}x^2+\frac{1}{2}N_{y0}y^2+N_{xy0}\,x\,y \tag{4.11}$$

where Y_{mn}, N_{x0}, N_{y0}, N_{xy0} are unknown functions of time just as X_{mn} is. Substituting Eqs. (4.10) and (4.11) into Eq. (4.8) and performing necessary integration gives expressions for N_{x0}, N_{y0}, N_{xy0} in terms of X_{mn} and Y_{mn} as follows:

$$\left.\begin{aligned}
N_{x0}&=\frac{\pi^2}{8(1-\nu^2)}\sum_{i,j=1}^{\infty}(i^2+\nu j^2)X_{ij}^2+\pi^2\sum_{i,j=1}^{\infty}j^2a_{ij}Y_{ij}\\
N_{y0}&=\frac{\pi^2}{8(1-\nu^2)}\sum_{i,j=1}^{\infty}(j^2+\nu i^2)X_{ij}^2+\pi^2\sum_{i,j=1}^{\infty}i^2a_{ij}Y_{ij}\\
N_{xy0}&=-\frac{\pi^2}{2(1+\nu)}\sum_{i,j=1}^{\infty}\sum_{k,l=1}^{\infty}i\,l\,b_{ij}b_{kl}X_{ij}X_{kl}
\end{aligned}\right\} \tag{4.12}$$

where

$$\left.\begin{aligned}
a_{ij}&=\int_0^1\sin i\,\pi\,x\,dx\int_0^1\sin j\,\pi\,x\,dx\\
b_{ij}&=\int_0^1\sin i\,\pi\,x\,\cos j\,\pi\,x\,dx
\end{aligned}\right\} \tag{4.13}$$

Substituting Eqs. (4.10), (4.11) and (4.12) into Eq. (4.5), multiplying $\sin m\pi x$ and $\sin n\pi y$, and then integrating yields

$$\left.\begin{aligned}
&\ddot{X}_{mn}+2\varepsilon\zeta\dot{X}_{mn}+p^2{}_{mn}X_{mn}-\varepsilon Q_{mn}\\
&\quad=\varepsilon\sum_{f,g=1}^{\infty}\sum_{\alpha,\beta=1}^{\infty}K_{mnfg\alpha\beta}Y_{fg}X_{\alpha\beta}\\
&\quad+\varepsilon\sum_{i,j=1}^{\infty}\sum_{k,l=1}^{\infty}\sum_{\alpha,\beta=1}^{\infty}L_{mnijkl\alpha\beta}X_{ij}X_{kl}X_{\alpha\beta}
\end{aligned}\right\} \tag{4.14}$$

$$Y_{mn}=\sum_{i,j=1}^{\infty}\sum_{k,l=1}^{\infty}M_{mnijkl}X_{ij}X_{kl}$$

where the concrete expressions of the coefficients are omitted. In Eq. (4.14), dot means differentiation with respect to time. Also, p_{mn} and Q_{mn} are the natural frequency of order (m,n) and the excitation force acting on that mode respectively, and are given as follows:

$$\left.\begin{aligned} &p^2_{mn}=m^2+n^2\\ &Q_{mn}=4\int_0^1\int_0^1 q(x,y,t)\sin m\pi x\,\sin n\pi y\,dx\,dy \end{aligned}\right\} \qquad (4.15)$$

Substituting the second equation in Eq. (4.14) into the first yields the required modal equations expressed in terms of X_{mn} as follows:

$$\left.\begin{aligned} &\ddot{X}_{mn}+2\varepsilon\zeta\dot{X}_{mn}+p^2_{mn}X_{mn}\\ &\qquad=\varepsilon\sum_{i,j=1}^{\infty}\sum_{k,l=1}^{\infty}\sum_{\alpha,\beta=1}^{\infty}N_{mnijkl\alpha\beta}X_{ij}X_{kl}X_{\alpha\beta}+\varepsilon Q_{mn} \end{aligned}\right\} \qquad (4.16)$$

It is noted from Eq. (4.16) that each mode is coupled by nonlinear terms with one another.

4. 3. Oscillations near the Primary Resonance Point

4. 3. 1. Analysis by the perturbation method

With use of the modal equations obtained in the preceding section, the response of the membrane to arbitrary excitation can be obtained. Here, the response to a harmonic excitation of the form $q=q(x,y)\cos\omega t$ is considered. The characteristics of oscillations when ω comes near a certain natural frequency are discussed by taking up a typical case.

The typical case taken up here is one in which the excitation frequency comes near the primary resonance point of order (1,2). Since $p_{21}=p_{12}$, this primary resonance point coincides with that of order (2,1). As to the excitation force, it is assumed that its distribution is symmetric with respect to the straight line $y=1/2$, which implies that $Q_{12}=0$.

To conduct numerical calculation it is assumed that the behavior of the system is governed mainly by the two modes of orders (1,2) and (2,1), and hence the unknown quantities except X_{21} and X_{12} in Eq. (4.16) can be neglected. Then the Eq. (4.16) is reduced to

$$\left.\begin{aligned} &\ddot{X}+2\varepsilon\zeta\dot{X}+p^2X=\varepsilon(NX^2+\tilde{N}\tilde{X}^2)X+\varepsilon Q\cos\omega t\\ &\ddot{\tilde{X}}+2\varepsilon\zeta\dot{\tilde{X}}+p^2\tilde{X}=\varepsilon(N\tilde{X}^2+\tilde{N}X^2)\tilde{X} \end{aligned}\right\} \qquad (4.17)$$

where

$$\left.\begin{aligned} &X=X_{21},\ \widetilde{X}=X_{12},\ Q\cos\omega t=Q_{21}\\ &N=N_{21212121}=N_{12121212}\\ &\widetilde{N}=N_{21211212}+N_{21122112}+N_{21121221}\\ &\quad=N_{12122121}+N_{12211221}+N_{12212112}\end{aligned}\right\} \tag{4.18}$$

It is assumed that the detuning betwen the excitation frequency ω and the natural frequency p is of the order of ε, and hence can be put in the form

$$\omega=p+\varepsilon\sigma \tag{4.19}$$

To solve Eq. (4.17), the perturbation method of multiple time scales[4] is employed and the solution is sought in the following form:

$$\left.\begin{aligned} &X=X_0(T_0,T_1,\cdot\cdot)+\varepsilon X_1(T_0,T_1,\cdot\cdot)+\cdots\cdot\\ &\widetilde{X}=\widetilde{X}_0(T_0,T_1,\cdot\cdot)+\varepsilon\widetilde{X}_1(T_0,T_1,\cdot\cdot)+\cdots\cdot\end{aligned}\right\} \tag{4.20}$$

solving Eq. (4.17) up to the order of ε yields the solution for X_0 and $\widetilde{X}_0$ as follows:

$$\left.\begin{aligned} &X_0=Ce^{i\sigma T_1}+\overline{C}e^{-i\sigma T_1}\\ &\widetilde{X}_0=De^{i\sigma T_1}+\overline{D}e^{-i\sigma T_1}\end{aligned}\right\} \tag{4.21}$$

where C, D are unknown functions of T_1, and $\overline{C}$, and $\overline{D}$ are their conjugates. These unknowns are determined from the conditions that X_1 and $\widetilde{X}_1$ have no secular terms, namely

$$\left.\begin{aligned} &2ipC'+2ip\zeta C-\frac{1}{2}Qe^{i\sigma T_1}\\ &\quad-N(3C^2\overline{C})-\widetilde{N}(2D\overline{D}C+D^2\overline{C})=0\\ &2ipD'+2ip\zeta D\\ &\quad-N(3D^2\overline{D})-\widetilde{N}(2C\overline{C}D+C^2\overline{D})=0\end{aligned}\right\} \tag{4.22}$$

where primes indicate differentiation with respect to time T_1.

To solve Eq. (4.22), C and D are put in the form

$$\left.\begin{aligned} &C=\frac{1}{2}Re^{i(\sigma T_1-\gamma)}\\ &D=\frac{1}{2}\widetilde{R}e^{i(\sigma T_1-\widetilde{\gamma})}\end{aligned}\right\} \tag{4.23}$$

and are substituted into Eq. (4.22), and then the resulting equations are separated into real and imaginary parts to yield

$$\left.\begin{aligned} pR' &= -p\zeta R+\frac{1}{2}Q\sin\gamma+\frac{1}{8}\tilde{N}\tilde{R}^2 R\sin(2\gamma-2\tilde{\gamma}) \\ pR\gamma' &= p\sigma R+\frac{1}{2}Q\cos\gamma+\frac{3}{8}NR^3+\frac{1}{8}\tilde{N}\tilde{R}^2 R\{2+\cos(2\gamma-2\tilde{\gamma})\} \\ p\tilde{R}' &= -p\zeta\tilde{R}+\frac{1}{8}\tilde{N}R^2\tilde{R}\sin(2\tilde{\gamma}-2\gamma) \\ p\tilde{R}\tilde{\gamma}' &= p\sigma\tilde{R}+\frac{3}{8}N\tilde{R}^3+\frac{1}{8}\tilde{N}R^2\tilde{R}\{2+\cos(2\tilde{\gamma}-2\gamma)\} \end{aligned}\right\} \quad (4.24)$$

To obtain steady-state solutions of Eq. (4.24), $R'=\tilde{R}'=\gamma'=\tilde{\gamma}'=0$ are substituted into it. Then the solutions of the obtained equations are substituted into Eq. (4.23), Eq. (4.21) and Eq. (4.10) successively to yield the solutions of Eq. (4.5) in the following form:

$$w=R\cos(\omega t-\gamma)\sin 2\pi x\sin\pi y+\tilde{R}\cos(\omega t-\tilde{\gamma})\sin\pi x\sin 2\pi y \quad (4.25)$$

The form of Eq. (4.24) reveals that it has two kinds of solutions. One is the solution of for which $\tilde{R}=0$, a natural consequence of $Q_{12}=0$, and hence this solution implies the occurrence of a usual harmonic oscillation. The other is the solution for which $\tilde{R}\neq 0$, which occurs due to the coupling by nonlinear terms, and this solution implies the occurrence of the oscillation containing the two modes with the same natural frequency.

The stability of a steady-state solution is determined by giving to the steady-state solution C, D a slight disturbance ΔC, ΔD, and examining its variation with respect to time. For this purpose, C and D in Eq. (4.22) are replaced by $C+\Delta C$ and $D+\Delta D$ respectively, and small quantities of the second order are neglected to yield the equations governing ΔC and ΔD. Then to transform the resulting equation in the form with real coefficients, ΔC and ΔD are replaced by

$$\left.\begin{aligned} \Delta C &= \frac{1}{2}(\zeta+i\eta)e^{i\sigma T_1} \\ \Delta D &= \frac{1}{2}(\tilde{\zeta}+i\tilde{\eta})e^{i\sigma T_1} \end{aligned}\right\} \quad (4.26)$$

and the resulting equations are separated into real and imaginary parts. Finally the eigenvalues of the last equations are determined and the stability is determined whether thier real parts are positive or nagative.

4. 3. 2. Characteristics of the oscillations

To discuss the characteristics of the oscillations, numerical calculation is conducted. For numerical calculation, it is assumed, in accordance with the experiment to be mentioned later, that the excitation force takes a constant value q_0 inside, and zero

outside, of a square whose side length is b_M and whose midpoint coincides with point (x_M, y_M). In Fig. 4. 1 is shown an example of the response curves and phase curves obtained for this case for values of parameters as given in the figure.

In the figures, solid and dotted lines indicate stable and unstable oscillations, respectively. From the figures it is seen that the response curves consist of two kinds of branches, one denoted by O_0 and O_2 for which $\widetilde{R}=0$, and the other for which $\widetilde{R}\neq 0$. Among the latter branches, the branches A and B are stable. The branch A bifurcates from branch O_0 and the bifurcating point coincides with the boundary point between stable and unstable regions of the branch O_0, while branch B exists separately from other branches.

The characteristics of oscillations obtained from Fig. 4. 1 is as follows. When, for example, the excitation frequency ω is increased gradually from lower values, the harmonic oscillation expressed by branch O_0 appears at first. When ω exceeds the value of ●, the oscillation expressed by branch A appears instead, in which $\widetilde{R}$ is large, and hence this oscillation consists of the two modes of orders (1,2) and (2,1). When ω

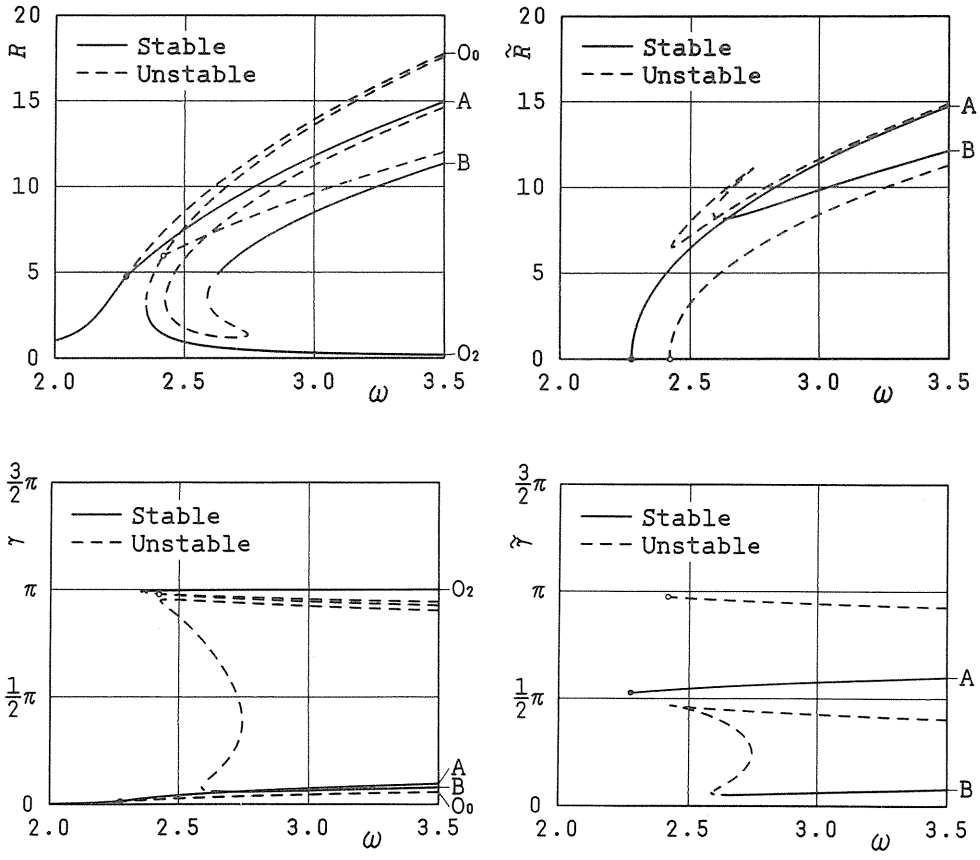

(ν=0.3, $2\varepsilon\zeta$=0.005, $\varepsilon=1\times10^3$, q_0=20, x_M=0.25, y_M=0.5, b_M=0.25)

Fig. 4. 1. Response and phase curves obtained theoretically.

increases further, R and $\widetilde{R}$ become almost the same values and at the same time the phase difference between the two modes is nearly $\pi/2$, as can be seen by comparing γ and $\widetilde{\gamma}$. Thus the last oscillation takes the form of rotary type of oscillation rotating with the angular velocity equal to the excitation frequency.

As mentioned above, branch B exists separately from other branches, so the oscillation represented by B doesn't occur when the excitation frequency is increased gradually, but occurs when appropriate initial conditions are given. For this oscillation, while R and $\widetilde{R}$ are almost the same value, the phase difference between the two modes is zero, which is different from that of branch A. Hence, this oscillation is not a rotary type, but one whose nodal line is placed along the diagonal line of the membrane. Thus, this is such a kind of oscillation that has no counterpart in the circular membrane.

4. 4. Experimental Analysis

4. 4. 1. Experimental method

To check the validity of the theoretical analysis presented in Sect. 4. 3, an experimental analysis was conducted by use of a thin steel square membrane. Schematic diagram of the experimental apparatus used in this study is shown in Fig. 4. 2. In this apparatus, the square membrane is fixed to four separate frames, and these frames are fixed to the outer frames through bolts. By revolving the bolts, the tension in the membrane can be adjusted.

Excitation force is given to the membrane by two electro-magnets put on both sides of the membrane and by flowing electric current into them alternately. The two electro-magnets are placed around point $x_M=3a/4$, $y_M=a/2$, so that $Q_{12}=0$ is valid.

To measure vibrations, two sensors are placed at points $x=a/4$, $y=a/2$ and $x=a/2$, $y=3a/4$. These points are on nodal lines of one mode or the other, so the two modes can be measured separately from each other.

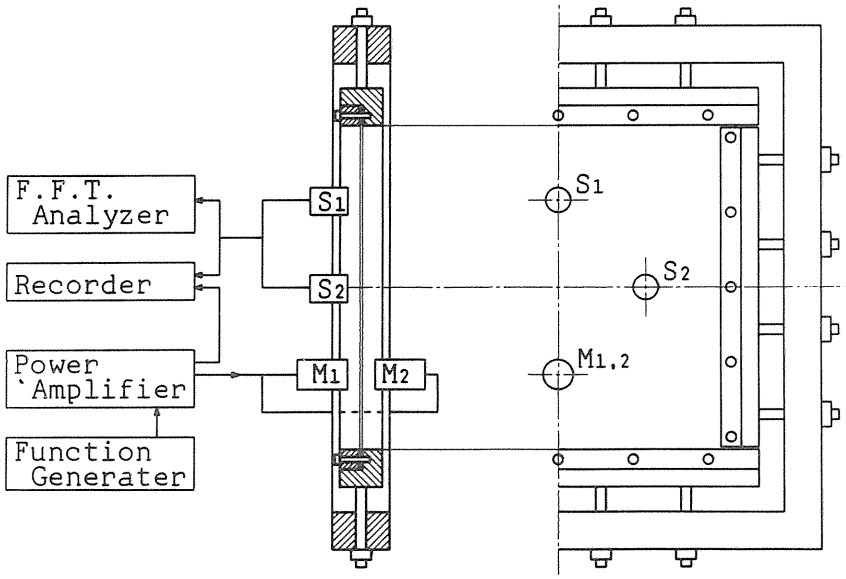

Fig. 4. 2. Schematic diagram of the experimental apparatus.

The dimensions and the physical properties of the membrane are as follows:

side length	$a=401$ mm
thickness	$h=0.25$ mm
Young's modulus	$E=206$ GPa
density	$\rho=7.7\times10^3$ Kg/m^3
Poisson's ratio	$\nu=0.3$

The natural frequencies obtained experimentally are

$$p_{21}=p_{12}=190 \text{ Hz}$$

4. 4. 2. Experimental results

By exciting the membrane by the excitation force with its frequency close to the natural frequency of order (1,2), two kinds of oscillations as shown in the left sides in (a) and (b) in Fig. 4. 3 was observed. In the figures, the upper and lower waves in each figure are the deflections at points $x=a/4$, $y=a/2$ and $x=a/2$, $y=3a/4$, respectively. When account is taken of the location of the sensors, the upper and lower waves can be considered to correspond to X and $\widetilde{X}$ in Eq. (4.10). In the right sides in Fig. 4. 3 are given Lissajous' figures obtained when deflections of upper and lower waves are taken as abscissa and ordinate. In Fig. 4. 4 is given response curves obtained experimentally. As in Fig. 4. 3, the amplitudes at points $x=a/4$, $y=a/2$ and $x=a/2$, $y=3a/4$ correspond to R and $\widetilde{R}$ in Eq. (4.25), and hence the response curves in Fig. 4. 4 correspond to those in Fig. 4. 1.

From Figs. 4. 3 and 4. 4, the following can be said as to the characteristics of the oscillation. When ω increases gradually from lower values, the oscillation represented by branch with notation I in Fig. 4. 4 appears at first. In this branch, the amplitudes of $\widetilde{R}$ is nearly zero for small excitation frequency but becomes large suddenly when the excitation frequency exceeds a certain value. The figure (a) in Fig. 4. 3 is the waves and the Lissajous' figure for the oscillation for large $\widetilde{R}$. From this figure it is seen that the phase difference between the two modes is nearly $\pi/2$. Thus it is seen that when the excitation frequency is small, the ordinary harmonic oscillation occurs, but as the excitation frequency becomes large the oscillation represented by branch A in Fig. 4. 1 occurs spontaneously.

In addition to branch I, there is one more branch denoted by II for which $\widetilde{R}\neq0$. The figure (b) in Fig. 4. 3 shows the waves and Lissajous' figure for the oscillation represented by branch II. As seen in the figure, the phase difference between the two modes is zero. Thus it is seen that the branch II corresponds to branch B in Fig. 4. 1.

From above it can be concluded that the experimental results confirm qualitatively the validity of the theoretical ones, except a slight disagreement which might be caused by nonuniformity of the tension or anisotropy of the membrane.

4. 5. Conclusions

A problem of nonlinear forced oscillation of a square membrane is considered. The problem taken up here concerns the oscillation of a membrane subjected to harmonic excitation near the primary resonance point of the natural mode with one nodal line. The

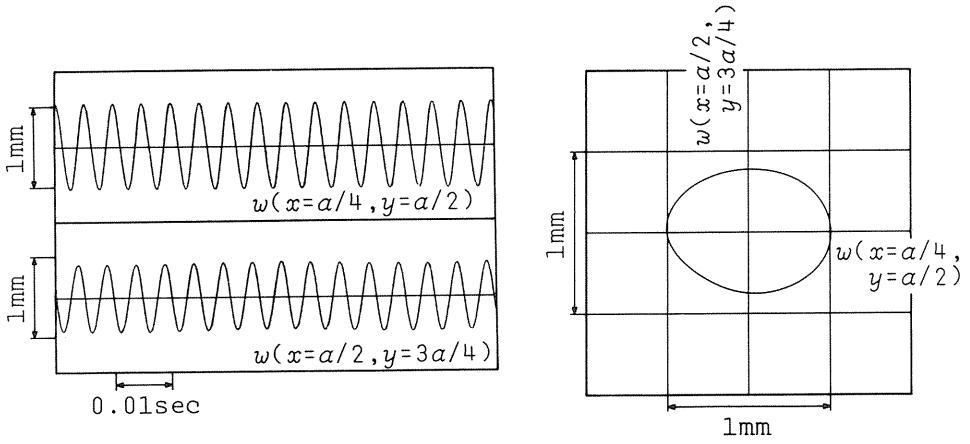

(a) Oscillation denoted by I in the Fig. 4. 4 (193.5 Hz).

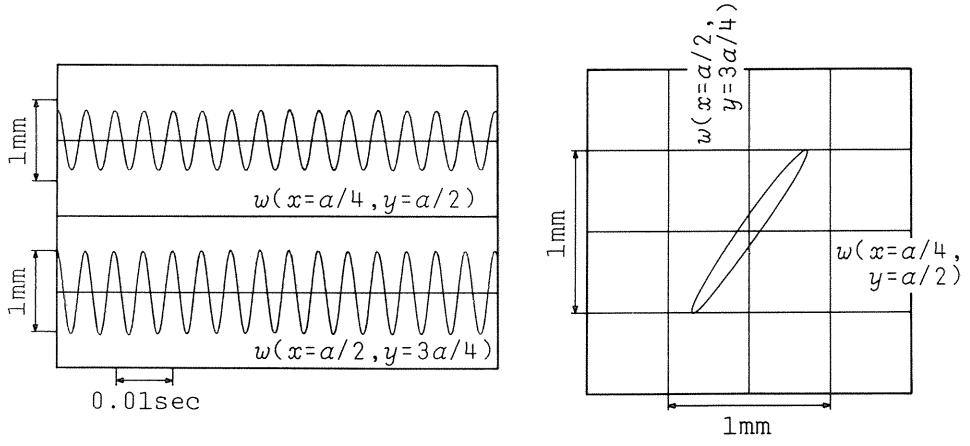

(b) Oscillation denoted by II in the Fig. 4. 4 (194.0 Hz).

Fig. 4. 3. Waveform and Lissajous' figure.

results obtained theoretically may be summarized as follows:

(1) According to the modal equations derived from the Karman-type equations of motion, the modes with the same natural frequency are generally coupled by nonlinear terms. Hence the two modes existing in pairs with the same natural frequency and the same mode shape are coupled by nonlinear terms.

(2) Hence in the membrane near the primary resonance point, in addition to the usual harmonic oscillation, the oscillations consisting of the two modes can be excited.

(3) The latter oscillations can be classified into two types. One is the oscillation for which the phase difference between the two modes is $\pi/2$. Hence this oscillation takes the form of the rotary type of oscillation rotating with the angular velocity equal to the

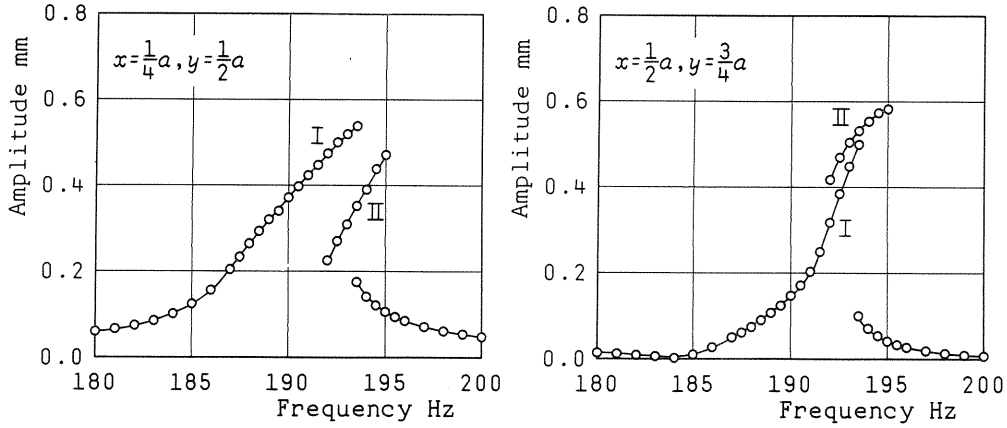

Fig. 4. 4. Response curves obtained experimentally.

excitation frequency.

(4) Another type of oscillation consisting of the two modes is the one for which the phase difference between the two modes is zero. When this oscillation occurs, the nodal line is placed at different position from that of the linear membrane. This oscillation has no counterpart in the circular membrane.

Thus it was shown theoretically that multi-mode response occurs in the square membrane.

Finally an experimental analysis is conducted, and the validity of the theoretical analysis is confirmed.

5. Multi-mode Response of a Beam between Bending and Twisting Modes

5. 1. Introduction

The problems of bending vibrations of a beam with large amplitudes have been the subject of many investigators.[40–48] One of the present authors also treated one such problem and showed that a multi-mode response can occur in a beam subjected to periodic excitation.[47–51]

Bending and twisting displacements may be coupled by nonlinear terms for large amplitudes in a beam with such a cross section for which they are not coupled for small amplitudes. Hence, it is expected that in such a beam, bending-twisting oscillations caused by nonlinear coupling may occur. However, it seems that the problems of this type of oscillation have scarcely been investigated.

In this chapter, the dynamic response of a beam with a thin rectangular cross section subjected to harmonic excitation in the lateral direction is taken up. The possibility of a multi-mode response between bending and twisting modes is discussed for the case in which one of natural frequencies of bending modes and one of those of twisting modes are in a certain relation.

For theoretical analysis, the equations of motion for the problem are obtained, from

which modal equations are derived. Then, the modal equations are solved by a perturbation method.[4] Finally, to confirm the validity of the theoretical analysis, an experimental analysis is conducted.

5. 2. *Fundamental Equations and The Modal Equations*

5. 2. 1. *Fundamental equations*

A beam with length l, width b and thickness h, and stretched in the axial direction by initial force N_0 is considered. For simplicity, it is assumed that $l \gg b \gg h$, and that both ends are simply supported. As shown in Fig. 5. 1, x, y and z axes are taken along the center line, in the direction of width and in the direction of thickness, respectively, of the beam in the equilibrium state. The displacement in the direction of x axis, deflection in the direction of z axis and the torsion around x axis are denoted by u, w and ϕ, respectively. The magnitudes of u, w and ϕ as well as their derivatives are assumed to be of the following order:

$$\left.\begin{array}{lll} w=O(1), & & \phi=O(1) \\ \dfrac{\partial w}{\partial x}=O(\varepsilon), & u=O(\varepsilon), & \dfrac{\partial \phi}{\partial x}=O(\varepsilon) \\ \dfrac{\partial^2 w}{\partial x^2}=O(\varepsilon^2), & \dfrac{\partial u}{\partial x}=O(\varepsilon^2), & \dfrac{\partial^2 \phi}{\partial x^2}=O(\varepsilon^2) \end{array}\right\} \tag{5.1}$$

Unit vectors e_x, e_y and e_z taken along x, y and z axes in the equilibrium state become, during motion, as follows:

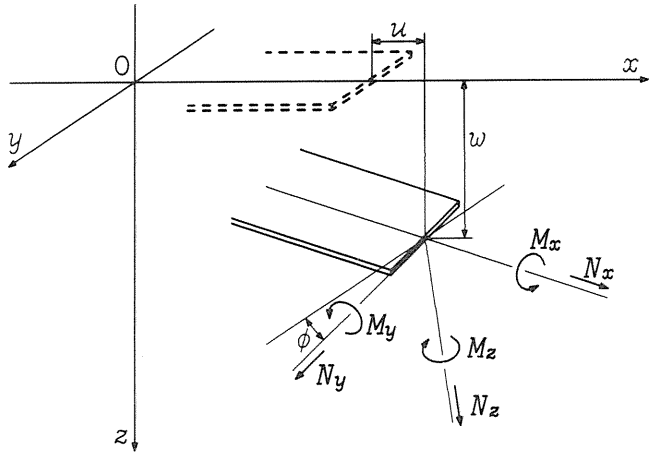

Fig. 5. 1. Coordinate system located in a beam.

$$\left.\begin{aligned} e'_x &= e_x + \frac{\partial w}{\partial x} e_z \\ e'_y &= e_y + \phi e_z \\ e'_z &= -\frac{\partial w}{\partial x} e_x - \phi e_y + e_z \end{aligned}\right\} \tag{5.2}$$

Hence, the position vector $\boldsymbol{R}$ of a point with coordinates (x,y,z) in the equilibrium state becomes, during motion, as follows:

$$\left.\begin{aligned} \boldsymbol{R} &= (x+u)e_x + we_z + ye'_y + ze'_z \\ &= (x+u-z\frac{\partial w}{\partial x})e_x + (y-z\phi)e_y + (z+w+y\phi)e_z \end{aligned}\right\} \tag{5.3}$$

Then the strain in the direction of x-axis becomes, when small quantities of higher order are neglected, as follows:

$$\left.\begin{aligned} \varepsilon_x &= \frac{1}{2}(\frac{\partial \boldsymbol{R}}{\partial x} \cdot \frac{\partial \boldsymbol{R}}{\partial x} - 1) \\ &\fallingdotseq \frac{\partial u}{\partial x} + \frac{1}{2}(\frac{\partial w}{\partial x})^2 + \frac{1}{2}(y^2+z^2)(\frac{\partial \phi}{\partial x})^2 - z\frac{\partial^2 w}{\partial x^2} + y\frac{\partial w}{\partial x} \cdot \frac{\partial \phi}{\partial x} \end{aligned}\right\} \tag{5.4}$$

Substituting this into the expression

$$\sigma_x = E\varepsilon_x + N_0/A \tag{5.5}$$

for stress in the direction of x-axis, and integrating the result over the cross section yields the resultant stress N_x and the resultant moments M_y, M_z as follows:

$$\left.\begin{aligned} N_x &= \int \sigma_x \, dA = N_0 + EA\{\frac{\partial u}{\partial x} + \frac{1}{2}(\frac{\partial w}{\partial x})^2\} + \frac{1}{2}EI_0(\frac{\partial \phi}{\partial x})^2 \\ M_y &= \int z\sigma_x \, dA = -EI_y \frac{\partial^2 w}{\partial x^2} \\ M_z &= -\int y\sigma_x \, dA = -EI_z \frac{\partial w}{\partial x} \cdot \frac{\partial \phi}{\partial x} \end{aligned}\right\} \tag{5.6}$$

Also the resultant moment around x-axis is obtained as follows:[52]

$$M_x = (GK_t + \bar{K})\frac{\partial \phi}{\partial x} \tag{5.7}$$

In Eqs. (5.6) and (5.7), E, G and A are the Young's modulus, the shear modulus of elasticity and the area of cross section, respectively. Furthermore, I_y, I_z, I_0 are moments of inertia, and K_t and K are the St. Venant twisting constant and the Wagner coefficient, respectively, and are defined as follows:

$$\left.\begin{aligned} &I_y=\int z^2 dA=\frac{1}{12}bh^3,\ I_z=\int y^2 dA=\frac{1}{12}hb^3 \\ &I_0=\int (y^2+z^2)dA\fallingdotseq I_z,\ K_t=\frac{1}{3}bh^3 \\ &\overline{K}=\int (y^2+z^2)\sigma_x\, dA\fallingdotseq\frac{I_0}{A}\{N_x+\frac{2}{5}EI_z(\frac{\partial\phi}{\partial x})^2\} \end{aligned}\right\} \tag{5.8}$$

The resultant stresses N_y and N_z, not defined in Eq. (5.6), are supposed to be determined from the condition of equilibrium.

The equations of motion derived in terms of resultant stresses and resultant moments given in Eqs. (5.6) and (5.7), with an inclusion of viscous damping forces, become as follows:

$$\left.\begin{aligned} &\frac{\partial}{\partial x}(N_x-N_z\frac{\partial w}{\partial x})=0 \\ &\frac{\partial}{\partial x}(N_z+N_x\frac{\partial w}{\partial x}+N_y\phi)=\rho A\frac{\partial^2 w}{\partial t^2}+c_x\frac{\partial w}{\partial x}-q \\ &\frac{\partial}{\partial x}(M_x-M_z\frac{\partial w}{\partial x})=\rho I_0\frac{\partial^2\phi}{\partial t^2}+c_y\frac{\partial\phi}{\partial x} \\ &\frac{\partial}{\partial x}(M_y-M_z\phi)=N_z \\ &\frac{\partial}{\partial x}(M_z+M_x\frac{\partial w}{\partial x}+M_y\phi)=N_y \end{aligned}\right\} \tag{5.9}$$

where ρ, c_x and c_y and q are the density, the damping coefficients, and the external force, respectively. To simplify the analysis, small quantities of higher orders are neglected. Then the first equation in Eq. (5.9) becomes

$$\frac{\partial}{\partial x}(N_x)=0 \tag{5.10}$$

implying that N_x is independent of x. With this taken into account, the first equation of Eq. (5.6) is solved with respect to u, under the boundary condition that $u=0$ on both edges, to yield

$$N_x=\overline{N}=N_0+\frac{E}{2l}\int_0^l\{A(\frac{\partial w}{\partial x})^2+I_0(\frac{\partial\phi}{\partial x})^2\}\,dx \tag{5.11}$$

Similarly, the forth and fifth of Eq. (5.9) give

$$\left.\begin{aligned} N_z &= -EI_y\frac{\partial^3 w}{\partial x^3}+EI_z\frac{\partial}{\partial x}\left(\frac{\partial w}{\partial x}\cdot\frac{\partial \phi}{\partial x}\phi\right) \\ N_y &= -EI_z\frac{\partial}{\partial x}\left(\frac{\partial w}{\partial x}\cdot\frac{\partial \phi}{\partial x}\right) \\ &\quad +\frac{\partial}{\partial x}\left\{\left(GK_t+\frac{I_0}{A}N_0\right)\frac{\partial w}{\partial x}\cdot\frac{\partial \phi}{\partial x}-EI_y\frac{\partial^2 w}{\partial x^2}\phi\right\} \end{aligned}\right\} \tag{5.12}$$

Substituting these into the second and third of Eq. (5.9) yields

$$\left.\begin{aligned} &\rho A\frac{\partial^2 w}{\partial t^2}+c_x\frac{\partial w}{\partial t}+EI_y\frac{\partial^4 w}{\partial x^4}+\bar{N}\frac{\partial^2 w}{\partial x^2}-q \\ &\quad =EI_z\frac{\partial}{\partial x}\left\{\frac{\partial w}{\partial x}\left(\frac{\partial \phi}{\partial x}\right)^2\right\}-EI_y\frac{\partial}{\partial x}\left\{\phi\frac{\partial}{\partial x}\left(\phi\frac{\partial^2 w}{\partial x^2}\right)\right\} \\ &\quad +\left(GK_t+\frac{I_0}{A}N_0\right)\frac{\partial}{\partial x}\left\{\phi\frac{\partial}{\partial x}\left(\frac{\partial w}{\partial x}\cdot\frac{\partial \phi}{\partial x}\right)\right\} \\ &\rho I_0\frac{\partial^2 \phi}{\partial t^2}+c_y\frac{\partial \phi}{\partial t}-\left(GK_t+\frac{I_0}{A}\bar{N}\right)\frac{\partial^2 \phi}{\partial x^2} \\ &\quad =EI_z\frac{\partial}{\partial x}\left\{\frac{\partial \phi}{\partial x}\left(\frac{\partial w}{\partial x}\right)^2\right\}+\frac{2}{5}EI_z\frac{I_0}{A}\frac{\partial}{\partial x}\left\{\left(\frac{\partial \phi}{\partial x}\right)^3\right\} \end{aligned}\right\} \tag{5.13}$$

Now, the nondimensional quantities

$$\left.\begin{aligned} &\varepsilon=\frac{A}{l^2},\quad x'=\frac{x}{l},\quad t'=\frac{\pi}{l}\sqrt{\frac{N_0}{\rho h}}t,\quad w'=\frac{2\pi}{l}\sqrt{\frac{AE}{\varepsilon N_0}}w \\ &\phi'=\frac{2\pi}{l}\sqrt{\frac{AE}{\varepsilon N_0}}\cdot\sqrt{\frac{I_z}{A}}\phi,\quad 2\varepsilon\zeta=\frac{lc_x}{\pi\sqrt{\rho A N_0}} \\ &2\varepsilon\zeta_y=\frac{lc_y}{\pi\sqrt{\rho A N_0}}\frac{A}{I_z},\quad \varepsilon q'=\frac{lq}{2\pi N_0}\sqrt{\frac{AE}{\varepsilon N_0}} \\ &\varkappa_0=\frac{GK_t}{N_0}\frac{A}{I_z},\quad \varkappa_1=\pi^2\frac{EI_y}{N_0 l^2},\quad \beta_1=\frac{I_y}{I_z},\quad \beta_2=\frac{GK_t}{EI_z}+\frac{N_0}{EA} \end{aligned}\right\} \tag{5.14}$$

are introduced. When these quantities are used, account is taken of the fact that $\beta_1 \ll 1$, $\beta_2 \ll 1$, and finally primes are omitted, Eq. (5.13) is rewritten as follows:

$$\left.\begin{aligned}
&\frac{\partial^2 w}{\partial t^2}+2\varepsilon\zeta_x\frac{\partial w}{\partial t}-\frac{1}{\pi^2}\left[1+\frac{2\varepsilon}{\pi^2}\int_0^1\{(\frac{\partial w}{\partial x})^2+(\frac{\partial \phi}{\partial x})^2\}\,dx\right]\frac{\partial^2 w}{\partial x^2}+\varkappa_1\frac{\partial^2 w}{\partial x^4}\\
&\quad=4\frac{\varepsilon}{\pi^4}\frac{\partial}{\partial x}\{\frac{\partial w}{\partial x}(\frac{\partial \phi}{\partial x})^2\}+\varepsilon q\\
&\frac{\partial^2 \phi}{\partial t^2}+2\varepsilon\zeta_y\frac{\partial \phi}{\partial t}-\frac{1}{\pi^2}\left[1+\varkappa_0+\frac{2\varepsilon}{\pi^2}\int_0^1\{(\frac{\partial w}{\partial x})^2+(\frac{\partial \phi}{\partial x})^2\}\,dx\right]\frac{\partial^2 \phi}{\partial x^2}\\
&\quad=4\frac{\varepsilon}{\pi^4}\frac{\partial}{\partial x}\{\frac{\partial w}{\partial x}(\frac{\partial \phi}{\partial x})^2\}+\frac{8}{5}\frac{\varepsilon}{\pi^4}\frac{\partial}{\partial x}\{(\frac{\partial \phi}{\partial x})^3\}
\end{aligned}\right\}\quad(5.15)$$

5. 2. 2. Modal equations

Unknown quantities w and ϕ are put, so as to satisfy the boundary conditions, in the following form:

$$\left.\begin{aligned}
w&=\sum_{n=1}^{\infty}X_n\sin n\,\pi\,x\\
\phi&=\sum_{n=1}^{\infty}Y_n\sin n\,\pi\,x
\end{aligned}\right\}\quad(5.16)$$

where X_n and Y_n express contribution of each mode to deflection and torsion, respectively. Substituting Eq. (5.16) into Eq. (5.15), multiplying $\sin n\pi x$ on both sides and integrating with respect to x from 0 to 1 yields, for determining X_n, Y_n, the following equations:

$$\left.\begin{aligned}
&\dot{X}_n+2\varepsilon\zeta_x\dot{X}_n+p_{n^2}X_n+\varepsilon n^2\sum_{m=1}^{\infty}m^2(X_m^2+Y_m^2)X_n\\
&\quad=-\varepsilon\sum_{ikl=1}^{\infty}H_{nijk}Y_iY_jX_k+\varepsilon Q_n\\
&\dot{Y}_n+2\varepsilon\zeta_y\dot{Y}_n+\tilde{p}_{n^2}Y_n+\varepsilon n^2\sum_{m=1}^{\infty}m^2(X_m^2+Y_m^2)Y_n\\
&\quad=-\varepsilon\sum_{ikl=1}^{\infty}H_{nijk}(X_iX_jY_k+\frac{2}{5}Y_iY_jY_k)
\end{aligned}\right\}\quad(5.17)$$

where

$$\left.\begin{aligned}
&p_n=n\sqrt{1+\varkappa_1 n^2},\quad \tilde{p}_n=n\sqrt{1+\varkappa_0}\\
&Q_n=2\int_0^1\int_0^1 q(x,t)\sin m\,\pi\,x\,dx\\
&H_{nijk}=8\int_0^1\cos n\,\pi\,x\cos i\,\pi\,x\cos j\,\pi\,x\cos k\,\pi\,x\,dx
\end{aligned}\right\}\quad(5.18)$$

From Eq. (5.17), it is noted that bending and twisting modes are coupled by nonlinear terms.

5. 3. Oscillations Near The Primary Resonance Point

5. 3. 1. Analysis by the perturbation method

The natural frequencies p_n and $\tilde{p}_n$ for bending and twisting modes of a beam are, as

already mentioned, given by Eq. (5.18). From this and Eq. (5.14), it is noted that the ratio of p_n and $\tilde{p}_n$ are varied with the initial tension N_0. Due to this, one of natural frequencies of bending modes coincide with some of those of twisting modes. Here is treated the case in which the natural frequency of the second bending mode coincides with that of the first twisting mode.

The excitation is supposed to be the harmonic one of the form $q=q(x)\cos\omega t$ and its frequency ω is near the primary resonance point of the natural frequencies mentioned above.

It is assumed for simplicity that the behavior of the system is governed mainly by the second bending mode and the first twisting mode, and thus the quantities other than X_2 and Y_1 can be neglected in Eq. (5.17). Then, Eq. (5.17) is reduced to

$$\left.\begin{aligned}&\ddot{X}+2\varepsilon\zeta_x\dot{X}+p^2X+\varepsilon(H_{xx}X^2+H_{xy}Y^2)X=\varepsilon Q\cos\omega\, t\\&\ddot{Y}+2\varepsilon\zeta_y\dot{Y}+p^2Y+\varepsilon(H_{yx}X^2+H_{yy}Y^2)Y=0\end{aligned}\right\}\tag{5.19}$$

where

$$\left.\begin{aligned}&X=X_2,\ Y=Y_1,\ p=p_2=\tilde{p}_1,\ Q\cos\omega\, t=q_2\\&H_{xx}=2^2\cdot 2^2,\ H_{xy}=2^2\cdot 1^2+H_{2112}\\&H_{yx}=1^2\cdot 2^2+H_{1221},\ H_{yy}=1^2\cdot 1^2+\frac{2}{5}H_{1111}\end{aligned}\right\}\tag{5.20}$$

It is also assumed that the detuning between the excitation frequency ω and the natural frequency p is of the order of ε, so that ω can be put in the form

$$\omega=p+\varepsilon\sigma\tag{5.21}$$

To solve Eq. (5.19) by the perturbation method of multiple time scales,[4] the solution is put in the form

$$\left.\begin{aligned}&X=X_0(T_0,T_1,\cdot\cdot)+\varepsilon X_1(T_0,T_1,\cdot\cdot)+\cdots\cdot\\&Y=Y_0(T_0,T_1,\cdot\cdot)+\varepsilon Y_1(T_0,T_1,\cdot\cdot)+\cdots\cdot\end{aligned}\right\}\tag{5.22}$$

where $T_0=t$, $T_1=\varepsilon t,\cdots$ are various times with different scales. Solving Eq. (5.19) within an accuracy of the order of ε yields the solution for X_0 and Y_0 as follows:

$$\left.\begin{aligned}&X_0=Ue^{i\sigma T_1}+\bar{U}e^{-i\sigma T_1}\\&Y_0=Ve^{i\sigma T_1}+\bar{V}e^{-i\sigma T_1}\end{aligned}\right\}\tag{5.23}$$

where U and V are unknown functions of T_1, and $\bar{U}$ and $\bar{V}$ are their conjugates. These unknown functions are determined from the conditions that X_1 and Y_1 have no secular terms; namely,

$$\left.\begin{aligned} &2ipU'+2ip\zeta_x U-\frac{1}{2}Qe^{i\sigma T_1}\\ &\quad+H_{xx}(3U^2\overline{U})+H_{xy}(2V\overline{V}U+V^2\overline{U})=0\\ &2ipV'+2ip\zeta_y V\\ &\quad+H_{yy}(3V^2\overline{V})+H_{yx}(2U\overline{U}V+U^2\overline{V})=0 \end{aligned}\right\} \tag{5.24}$$

where primes indicate differentiation with respect to time T_1.

To solve Eq. (5.24), U and V are put in the form

$$\left.\begin{aligned} U&=\frac{1}{2}Re^{i(\sigma T_1-\gamma)}\\ V&=\frac{1}{2}Se^{i(\sigma T_1-\delta)} \end{aligned}\right\} \tag{5.25}$$

Substituting this into Eq. (5.24) and separating the resulting equations into real and imaginary parts yields

$$\left.\begin{aligned} pR'&=-p\zeta_x R+\frac{1}{2}Q\sin\gamma-\frac{1}{8}H_{xy}S^2R\sin(2\gamma-2\delta)\\ pR\gamma'&=p\sigma R+\frac{1}{2}Q\cos\gamma-\frac{3}{8}H_{xx}R^3\\ &\quad-\frac{1}{8}H_{xy}S^2R\{2+\cos(2\gamma-2\delta)\}\\ pS'&=-p\zeta_y S-\frac{1}{8}H_{yx}R^2S\sin(2\delta-2\gamma)\\ pS\delta'&=p\sigma S-\frac{3}{8}H_{yy}S^3-\frac{1}{8}H_{yx}R^2S\{2+\cos(2\delta-2\gamma)\} \end{aligned}\right\} \tag{5.26}$$

To obtain steady-state solutions of Eq. (5.26), $R'=S'=\gamma'=\delta'=0$ are substituted into it. Then, the solutions of the resulting equations are substituted into Eqs. (5.25), (5.23) and then (5.16) successively to yield the solution of Eq. (5.15) in the form:

$$\left.\begin{aligned} w&=R\cos(\omega t-\gamma)\sin 2\pi x\\ \phi&=S\cos(\omega t-\delta)\sin\pi x \end{aligned}\right\} \tag{5.27}$$

The form of Eq. (5.26) reveals that it has two kinds of solutions. One is the solution for which $S=0$, which implies the occurrence of the usual harmonic oscillation. The other is the solution for which $S\neq 0$, which implies the occurrence of not only the bending but also the twisting modes, i.e., the occurrence of the multi-mode response.

The stability of a steady-state solution U and V is determined by giving it a slight disturbance ΔU and ΔV, and examining its variation with respect to time. For this purpose, U and V are replaced in Eq. (5.24) by $U+\Delta U$ and $V+\Delta V$, respectively, and small quantities of the second order are neglected to obtain the equations governing ΔU and ΔV. Then, to transform the resulting equations in the form with real coefficients, ΔU and ΔV are replaced by

$$\left.\begin{aligned}\Delta U&=\frac{1}{2}(\xi+i\eta)e^{i\sigma T_1}\\ \Delta V&=\frac{1}{2}(\tilde{\xi}+i\tilde{\eta})e^{i\sigma T_1}\end{aligned}\right\} \tag{5.28}$$

and the obtained equation is separated into real and imaginary parts. Finally, the eigenvalue of the last equations are obtained and the stability is determined, whether their real parts are positive or nagative.

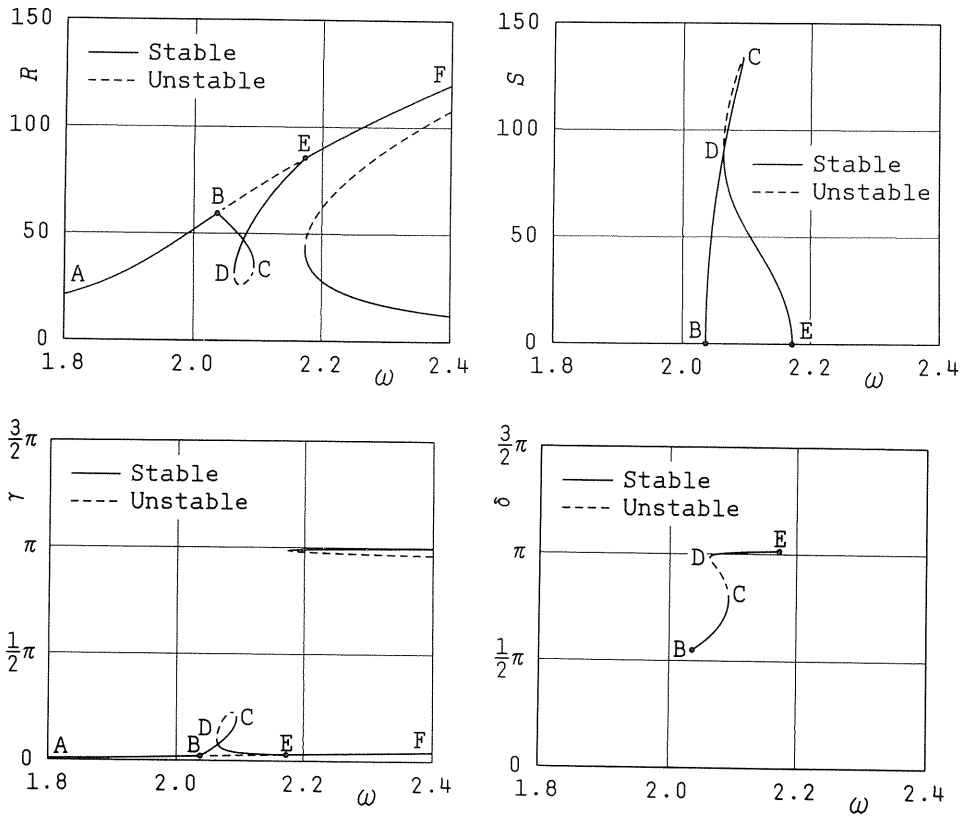

(p=2.01, $2\varepsilon\zeta_x=2\varepsilon\zeta_y$=0.01, $\varepsilon=1\times10^{-5}$, q_0=40, x_M=0.25, b_M=0.12)

Fig. 5. 2. Response and phase curves obtained theoretically.

5. 3. 2. Characteristics of the oscillations

To discuss the characteristics of the oscillations, numerical calculations are conducted. For this, it is assumed that the amplitude of the excitation force takes, in accordance with the experiments to be mentioned later, a constant value q_0 inside, and zero outside, of the region of the beam whose length is b_M and whose midpoint is $x=x_M$. In Fig. 5. 2 is shown an example of the response curve and phase curve obtained for this case for suitable values of the parameters.

In the figure, solid and dotted lines indicate stable and unstable oscillations, respectively. From this figure, it is seen that the response curve consists of two kinds of branches, one expressing the usual harmonic oscillations with $S=0$ and the other denoted by BCDE with $S\neq 0$. On the former branch ABEF exists unstable region BE, from whose boundary points, the branch BCDE bifurcates. On branch BCDE exist stable portions BC and DE.

The characteristics of oscillations can be discussed by Fig. 5. 2. When, for example, the excitation frequency ω is increased gradually from lower values, the harmonic oscillation expressed by branch AB first appears. When ω exceeds the value of point B, the harmonic oscillation is replaced by the oscillation expressed by branch BC with S increasing rapidly, and thus the multi-mode response of the bending and twisting modes occurs. The phase difference between these two modes is nearly $\pi/2$, as can be obtained by comparing γ and δ in Fig. 5. 2. When ω is further increased in this oscillatory state, jump phenomena occur at point C, and the oscillation expressed by branch DE appears. The phase difference between the two modes of this oscillation is nearly. With further increase of ω, R increases but S decreases. At point E, S finally becomes zero, and the harmonic oscillation expressed by branch EF appears.

5. 4. Experimental Analysis

5. 4. 1. Experimental method

To check the validity of the theoretical analysis presented in Sect. 5. 3, an experimental analysis was conducted with use of a steel beam. A schematic diagram of the experimental apparatus used in this study is shown in Fig. 5. 3. In this apparatus, the initial tension in the axial direction is given by the nut in the left side. The excitation is given to the beam by flowing electric current alternately into two electro-magnets placed on either side of the beam. To measure the deflection and the torsion separately, two sensors are put in the direction of the width of the beam as shown in the lower part of Fig. 5. 3, and the sum and the difference of the signals of each sensors are calculated by operational amplifiers.

The dimensions and the physical properties of the beam are as follows:

length	$l=1000$ mm
width	$b=32$ mm
thickness	$h=0.5$ mm
Young's modulus	$E=206$ GPa
shear modulus	$G=79.2$ GPa
density	$\rho=7.7\times10^3$ Kg/m^3

The position of the electro-magnets is $x_M=250$ mm, and the distance between the two

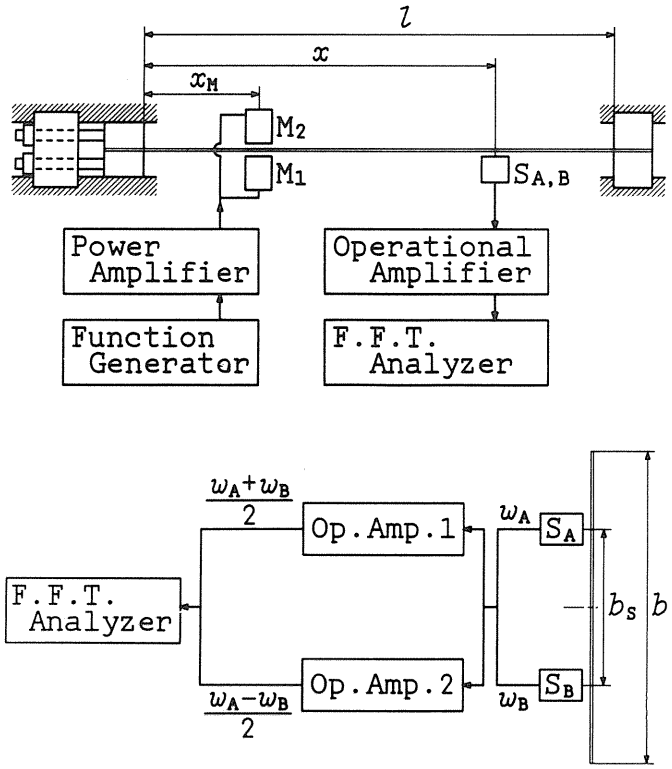

Fig. 5. 3. Schematic diagram of the experimental apparatus.

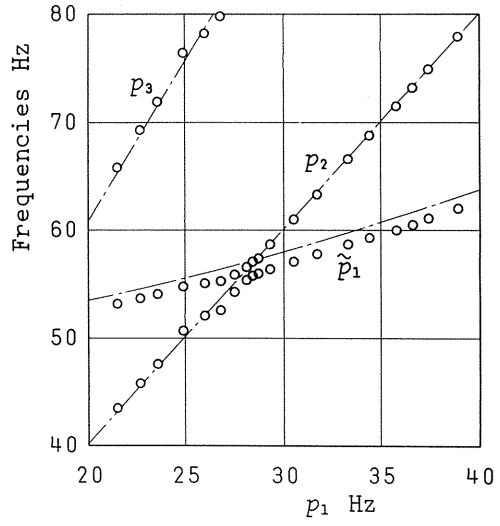

Fig. 5. 4. Natural frequencies of a beam.

sensors is 18 mm.

The natural frequencies of the beam obtained by varying the initial tension in the axial direction is as shown in Fig. 5. 4. In the figure, instead of the initial tension, the natural frequency of the first bending mode is taken as abscissa. For comparison, theoretical values are also shown by chain lines. From the figure, it is noted that for p_1=28 Hz the natural frequency of the second bending mode coincides with that of the first twisting mode, whose value is nearly 56 Hz.

5. 4. 2. Experimental results

The beam was excited with the excitation frequency nearly equal to the coincided natural frequencies. It was found that in addition to the usual harmonic oscillation, two kinds of oscillations as shown in Figs. 5. 5(a) and (b) occurred. In these figures, w_A and w_B are waves obtained by sensors A and B, and $(w_A+w_B)/2$ and $(w_A-w_B)/2$ are the calculated waves corresponding to deflection and torsion. In each figure of (a) and (b), the left and right waves are ones obtained at points $x=l/2$ and $x=3l/4$. From these figures, it is found that the oscillation containing twisting mode in fact occurs, and that the deflection takes the second mode shape and the torsion the first mode shape. In Fig. 5. 6

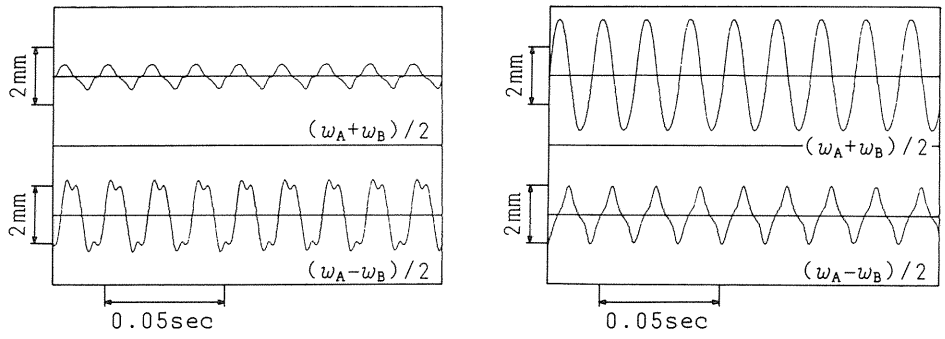

(a) Oscillation denoted by I in the Fig. 5. 6 (57.2 Hz).

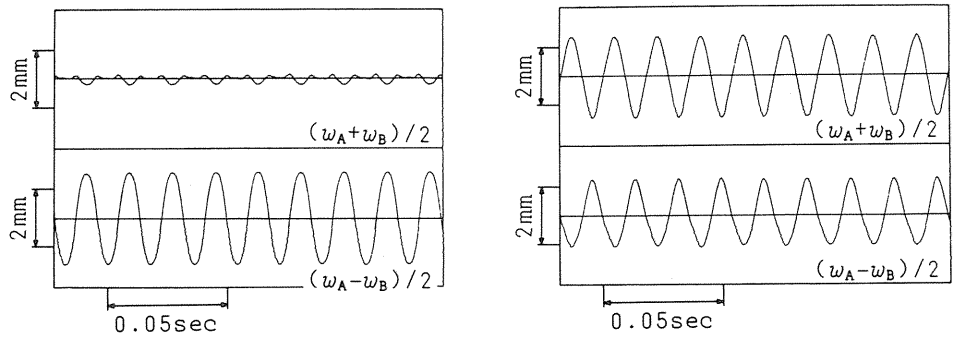

(b) Oscillation denoted by II in the Fig. 5. 6 (58.0 Hz).

Fig. 5. 5. Waveform.

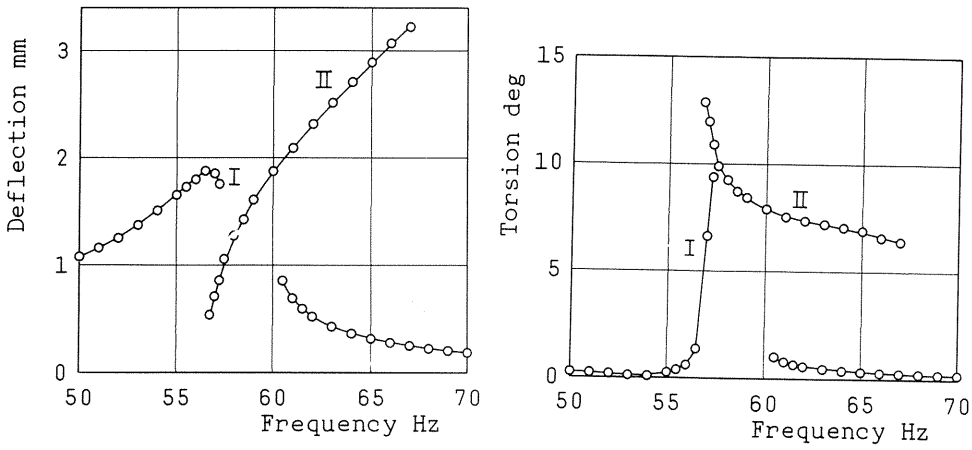

Fig. 5. 6. Response curves obtained experimentally.

are shown the response curves obtained experimentally at point $x=2l/3$.

From Figs. 5. 5 and 5. 6, the following is noted. When the excitation frequency is increased, the harmonic oscillation first appears. When the excitation frequency become higher than a certain value, the twisting mode increases rapidly and the oscillation represented by branch I occurs. As obtained from Fig. 5. 5, the phase difference between the bending and twisting modes of this oscillation is nearly $\pi/2$. Thus, the oscillation represented by branch I corresponds to that represented by branch BC of Fig. 5. 2.

When the excitation frequency is further increased in Fig. 5. 6, jump phenomena occur at a certain frequency and above that frequency the oscillation represented by branch II occurs. In this oscillatory state, the bending mode increases and twisting mode decreases with the excitation frequency. Furthermore in this state, the phase difference between the bending and twisting mode is nearly π. Thus, the oscillation represented by branch II corresponds to that of branch DE in Fig. 5. 2.

It is noted from Fig. 5. 5 that the oscillation represented by branch I contains higher harmonics, and to carry the analysis in more detail, higher modes should be taken into account. But this has not been done here.

In conclusion, the results of the experimental analysis confirmed qualitatively those of the theoretical analysis.

5. 5. *Conclusions*

As a problem of nonlinear bending-twisting oscillations of a beam, the dynamic response of a beam with a thin rectangular cross section to harmonic excitation in the lateral direction is considered. The case treated here is one in which the natural frequency of the second bending mode coincides with that of the first twisting mode, and in which the excitation is near these coincided natural frequencies. The obtained results may be summarized as follows.

(1) The equations of motion for the problem are obtained, from which modal equations are derived.

(2) The modal equations thus obtained reveal that the bending modes and the twisting modes are coupled by nonlinear terms.

(3) Due to this, the twisting modes occur in a certain region of the excitation frequency, although the excitation is in the lateral direction, and thus the multi-mode response occurs.

(4) There are two kinds oscillatory states in the multi-mode response. For one, the phase difference between the bending mode and the twisting mode is $\pi/2$, and for the other it is π. In the former oscillatory state, amplitudes of the twisting mode increase, but in the latter they decrease, as the excitation frequency increases.

Finally, the experimental analysis is conducted and the validity of the theoretical analysis is confirmed.

Reference

1) Eisley,J.G., Appl. Mech. Surveys, (1966), 285.
2) Sathyamoorthy,M and K.A.V.Pandalai, J.Aeronaut. soc. India, 24, (1972), 409.
3) Sathyamoorthy,M and K.A.V.Pandalai, J.Aeronaut. soc. India, 25, (1973), 1.
4) Nayfeh,A.H. and Mook,D.T. "Nonlinear Oscillations", JOHN WILEY & SONS, (1979).
5) Sathyamoorthy, Appl. Mech. Rev. 40–11, (1987), 1553.
6) Malkin,I.G., "Some Problems in the Theory of Nonlinear Oscillations", (1959), GITTL, Moscow.
7) Yamamoto,T., Yasuda,K. and Nagasaka,I., Bull. JSME 19, (1976), 1442.
8) Tondl.A., National Research Institute for Machine Design, (1972), Bechovice, Czechoslovakia.
9) Yamamoto,T., Yasuda,K. and Nakamura,T., Bull. JSME 17, (1974), 560.
10) Tiwari,R.N and Subramaian,R., J. Sound Vib., 47, (1976), 501.
11) Mojaddidy,Z., Mook,D.T. and Nayfeh,A.H., Proc. Sixth Canadian Congress Appl. Mech., 6, (1977), 387.
12) Dallos,P.J. and Linnell,C.O., J. Acoust. Soc. Am., 40, (1966), 561.
13) Dallos,P.J. and Linnell,C.O., J. Acoust. Soc. Am., 40, (1966), 4.
14) Dallos,P.J., J. Acoust. Soc. Am., 40, (1966), 1381.
15) Luukkala,M., Phys. Lett., 25a, (1967), 76.
16) Adler,L. and M.A.breazeale, J. Acoust. Soc. Am., 48, (1970), 1077.
17) Eller,A.I., J. Acoust. Soc. Am., 53, (1973), 758.
18) Yamamoto,T., Mem. Fac. Eng. Nagoya Univ., 9, (1957), 19.
19) Yamamoto,T., Bull. JSME, 4, (1961), 51.
20) Yamamoto,T., Bull. JSME, 4, (1961), 658.
21) Yamamoto,T. and Yasuda,K., J. Appl. Mech., 41, (1974), 781.
22) Yasuda,K. and Torii,T., Bull. JSME, 28–245, (1985), 2699.
23) Yasuda,K. and Torii,T., Bull. JSME, 29–250, (1985), 1253.
24) Yasuda,K. and Torii,T., Bull. JSME, 29–255, (1986), 3096.
25) Yasuda,K. and Uno,H., Bull. JSME, 26–216, (1983), 1050.
26) Yasuda,K. and Torii,T., JSME J. Int., 30–264, (1987), 963.
27) Carrier,G.F., Q. Appl. Math., 3–2, (1945), 157.
28) Oplinger,D.W., J. Acous. Soc. Am., 32–12, (1960), 1529.
29) Anand,G.V., J. Acous. Soc. Am., 45–5, (1969), 1089.
30) Eringen,A.C., Proc. 1st U.S.Nati. Cong. Appl. Mech., (1951), 139.
31) Chobotov,V.A. and Binder,R.C., J. Acoust. Soc. Am., 36–1, (1964), 59.
32) Keller,J.B. and Ting,L., Commun. Pure Appl. Math., 19–4, (1966), 371.
33) Mack,L.R. and McQueary,C.E., J. Acoust. Soc. Am., 42–1, (1967), 60.
34) Yen,D.H.Y. and Lee,T.W., Int. J. Non-Linear Mech., 10–1, (1975), 47.
35) Jones,R., Int. J. Non-Linear Mech., 9–2, (1974), 141.
36) Mazumdar,J. and Jones,R., J. Sound and Vib. 50–3, (1977), 389.

37) Yasuda,K. and Asano,T., Bull. JSME, 29–255, (1986), 3090.
38) Boltin,V.V., Nonconservative Problems in the Theory of Elastic Stability, (1963), 274, The Macmillan Co.
39) Evensen,D.A., J. Acoust. Soc. Am., 44–1, (1968), 84.
40) Ray,L.D. and Bert,C.W., Trans. ASME ser. B 91–4, (1969), 997.
41) Tseng,W.Y. and Dugundji,J., J. Appl. Mech., 37–2, (1970), 292.
42) Bennett,J.A. and Eisley,J.G., AIAA J., 8, (1970), 734.
43) Eisley,J.G., and Bennett,J.A., Int. J. Non-Linear Mech., 5, (1970), 645.
44) Tseng,W.Y. and Dugundji,J., J. Appl. Mech., 38–2, (1971), 467.
45) Busby,H.R.Jr. and Weingarten,J., Int. J. Non-Linear Mech., 7, (1972), 289.
46) Nayfeh,A.H., Mook,D.T. and Sridhar,S., J. Acoust. Soc. Am., 52–2, (1974), 281.
47) Bennett,J.A., AIAA J., 11, (1973), 710.
48) Nayfeh,A.H., Mook,D.T. and Lobitz,D.W., AIAA J., 12–9, (1974), 1222.
49) Yamamoto,T., Yasuda,K. and Aoki,K, Bull. JSME, 24, (1981), 1011.
50) Yamamoto,T., Yasuda,K. and Tei,N., Bull. JSME, 24, (1981), 1214.
51) Yamamoto,T., Yasuda,K. and Tei,N., Bull. JSME, 25, (1982), 959.
52) Chen,W.F. and Atsuta,T., "Theory of Beam-Columns, vol.1," (1976), McGraw-Hill, New York.